Science of the Total Environment 859 (2023) 160202

Contents lists available at ScienceDirect

Science of the Total Environment

journal homepage: www.elsevier.com/locate/scitotenv

Environmental controllers for carbon emission and concentration patterns in Siberian rivers during different seasons

Ivan V. Krickov [a], Artem G. Lim [a], Liudmila S. Shirokova [b,c], Mikhail A. Korets [d], Jan Karlsson [e], Oleg S. Pokrovsky [b,*]

[a] BIO-GEO-CLIM Laboratory, Tomsk State University, Tomsk 634050, Russia
[b] Geosciences and Environment Toulouse, UMR 5563 CNRS, Univeristy of Toulouse, 14 Avenue Edouard Belin, 31400 Toulouse, France
[c] N. Laverov Federal Center for Integrated Arctic Research, Russian Academy of Sciences, Arkhangelsk 163000, Russia
[d] V.N. Sukachev Institute of Forest, Siberian Branch of Russian Academy of Sciences, Krasnoyarsk 660036, Russia
[e] Climate Impacts Research Centre (CIRC), Department of Ecology and Environmental Science, Umeå University, Linnaeus väg 6, 901 87 Umeå, Sweden

HIGHLIGHTS

- The river size (6 order of magnitude in watershed area) had weak impact on CO_2 fluxes.
- CO_2 concentration and emission decreased from spring to summer and autumn.
- Lack of diel CO_2 variation in rivers
- Terrestrial DOC and POC may control C emission from small rivers.
- C emission from river surfaces was comparable to dissolved and particulate C export by rivers.

GRAPHICAL ABSTRACT

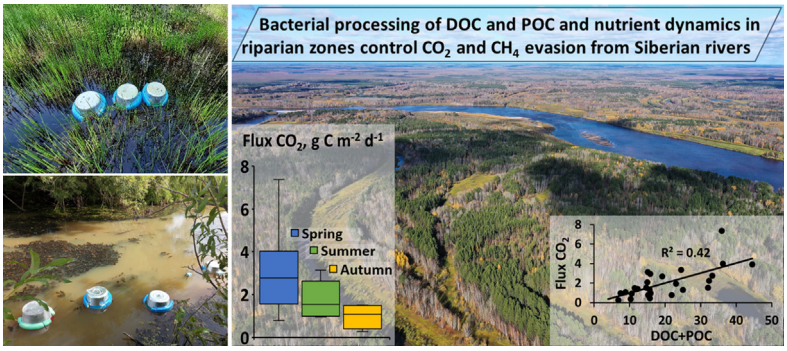

ARTICLE INFO

Editor: Ashantha Goonetilleke

Keywords:
CO_2
CH_4
Emission
Boreal
River
Organic carbon
Landscape

ABSTRACT

Despite the importance of small and medium size rivers of Siberian boreal zone in greenhouse gases (GHG) emission, major knowledge gaps exist regarding its temporal variability and controlling mechanisms. Here we sampled 11 pristine rivers of the southern taiga biome (western Siberia Lowland, WSL), ranging in watershed area from 0.8 to 119,000 km^2, to reveal temporal pattern and examine main environmental controllers of GHG emissions from the river water surfaces. Floating chamber measurements demonstrated that CO_2 emissions from water surface decreased by 2 to 4-folds from spring to summer and autumn, were independent of the size of the watershed and stream order and did not exhibit sizable (>30 %, regardless of season) variations between day and night. The CH_4 concentrations and fluxes increased in the order "spring ≤ summer < autumn" and ranged from 1 to 15 μmol L^{-1} and 5 to 100 mmol m^{-2} d^{-1}, respectively. The CO_2 concentrations and fluxes (range from 100 to 400 μmol L^{-1} and 1 to 4 g C m^{-2} d^{-1}, respectively) were positively correlated with dissolved and particulate organic carbon, total nitrogen and bacterial number of the water column. The CH_4 concentrations and fluxes were positively correlated with phosphate and ammonia concentrations. Of the landscape parameters, positive correlations were detected between riparian vegetation biomass and CO_2 and CH_4 concentrations. Over the six-month open-water period, areal emissions of C (>99.5 % CO_2; <0.5 % CH_4) from the watersheds of 11 rivers were equal to the total downstream C export in this part of the WSL. Based on correlations between environmental controllers (watershed land cover and the water column parameters), we hypothesize that the fluxes are largely driven by riverine mineralization of terrestrial dissolved and particulate OC, coupled with respiration at the river bottom and riparian sediments. It follows that, under climate

* Corresponding author.
E-mail address: oleg.pokrovsky@get.omp.eu (O.S. Pokrovsky).

http://dx.doi.org/10.1016/j.scitotenv.2022.160202
Received 12 September 2022; Received in revised form 11 November 2022; Accepted 11 November 2022
Available online 14 November 2022

warming scenario, most significant changes in GHG regimes of western Siberian rivers located in permafrost-free zone may occur due to changes in the riparian zone vegetation and water coverage of the floodplains.

1. Introduction

The greenhouse gas (GHG) emissions from rivers of boreal zone (Koprivnjak et al., 2010; Campeau and del Giorgio, 2014; Chadburn et al., 2017; Vonk et al., 2019; Vachon et al., 2021) have been estimated to play an important role in the carbon (C) cycle (Stackpoole et al., 2017; Tranvik et al., 2018; Karlsson et al., 2021). The global C emissions from rivers and streams range from 0.6 to 1.8 Pg C y^{-1} (Raymond et al., 2013; Lauerwald et al., 2015), which correspond to a non-negligible fraction (10 to 20 %) of total anthropogenic emissions. The atmospheric C fluxes from the river surfaces are fairly well studied in the European and North American boreal zone (Dawson et al., 2004; Dinsmore et al., 2009, 2013; Teodoru et al., 2009; Butman and Raymond, 2011; Wallin et al., 2013; Campeau et al., 2014; Leith et al., 2015; Rocher-Ros et al., 2019; Bretz et al., 2021; Pearce et al., 2022), and some Arctic and subarctic rivers of Alaska (Striegl et al., 2012; Crawford et al., 2013; Stackpoole et al., 2017). Although high latitude regions currently play a sub-ordinary role in global riverine CO_2 emissions (30 % temperate, 13 % Arctic regions, Liu et al., 2022), these territories are important because of their large C stocks, partly located in the permafrost, and their extreme vulnerability to observed and projected warming, which can release 80 Pg C upon abrupt thaw and up to 200 Pg C upon gradual thaw by 2300 (Turetsky et al., 2020). However, there are serious biases in geographical coverage of the land in terms of directly measured fluvial GHG concentrations and fluxes.

Among the boreal and subarctic regions, Siberia remains probably less studied due to logistic difficulties of conducting seasonal investigations with sufficient spatial coverage in this vast and often highly remote territory. Although recent progress in Western and Eastern Siberia allowed first-order assessment of riverine C export and emission fluxes (Denfeld et al., 2013; Serikova et al., 2018; Pokrovsky et al., 2020; Vorobyev et al., 2021; Krickov et al., 2021; Castro-Morales et al., 2022), further high spatial and seasonal resolution measurements of GHG concentration and fluxes of these underrepresented regions are needed. Under on-going climate warming, these organic C-rich regions may become a cornerstone in large-scale natural response (in terms of C emission and uptake) to rising water and soil temperatures (Chen et al., 2021), change of the hydrological regime (Bring et al., 2016), increase in plant biomass and northward shift of biome boundaries (Rosbakh et al., 2021). In particular, among various peatland-dominated small river catchments of the subarctic zone, those of the taiga region of the western Siberian Lowland (WSL) demonstrate most significant increase in water discharge, chiefly because rates of climate warming in this region are highest (Mack et al., 2021). It is expected that the changes of hydrological regime of large northern peatlands may induce sizable modification of both export (Frey and Smith, 2005; Pokrovsky et al., 2020) and emissions (Karlsson et al., 2021). The WSL inland waters act as a major regulator of GHG exchange with atmosphere, given that the current annual C (CO_2 + CH_4) emissions from this territory (lakes and rivers together) amount to 0.1 Pg C y^{-1}, which largely exceeds (7 to 9 times) C export to the Arctic Ocean and reach nearly half of the region's land uptake (Karlsson et al., 2021). However, the main environmental factors that govern the CO_2 and CH_4 evasion from fluvial systems of this region remain poorly known. This gap in knowledge does not allow foreseeing possible future changes in fluvial C export and emission in this region, which is subjected to strong environmental changes due to climate warming and likely act as major regulator of GHG fluxes between the land and the atmosphere in Northern Eurasia.

Towards better understanding of the magnitude of C transport and emission and main physico-chemical and landscape controllers for the C cycle of pristine river watersheds of contrasted land cover, we selected a suite of small to medium-size rivers of the WSL non-permafrost zone. We studied both GHG concentrations and CO_2 emission over 3 main hydrological seasons, including the day/night period. We hypothesized, first, that microbial processing and photodegradation of particulate and dissolved organic carbon (POC and DOC, respectively) in the water column are important drivers of CO_2 and CH_4 supersaturation of the river waters. This has been shown on a number of rivers in western Europe and Northern American regions (Battin et al., 2009; Vonk et al., 2015; Attermeyer et al., 2018) but hast not been tested in the vast territory of Siberian riverine network. Thus, a local maximum of POC concentration in WSL rivers located at the permafrost thaw boundary (Krickov et al., 2018) can tentatively explain elevated CO_2 emissions observed in this part of the WSL, discontinuous to sporadic permafrost zone (Serikova et al., 2018).

Our second hypothesis was that watershed size and OC quality exert important control on aquatic CO_2 and CH_4 emission, in accordance with studies of other regions (Hotchkiss et al., 2015). Indeed, it is quite frequent that lower order streams show higher CO_2 concentrations and emissions than the higher order rivers (Butman and Raymond, 2011). In the WSL, we thus expect variations of CO_2 per stream size, with small systems showing higher values than large systems as predicted conceptually (Hotchkiss et al., 2015) and verified at the basin-scale of other regions (e.g. Borges et al., 2015). The main reason for systematically higher CO_2 concentration and flux in small tributaries compared to the main stem is that the former are fed by mire waters with 'non-processed' organic matter, suitable for microbial degradation and leading to enhanced CO_2 production in the water column (i.e., Lim et al., 2022). Up to present time, these drivers of CO_2 emission were tested in temperate and boreal regions, however, it remains totally unknown, to which degree these factors can operate in the largest lowland in the world.

Third, we expected that diel variations in concentration and fluxes of CO_2 are mostly pronounced during summer/autumn period compared to the spring flood, due to enhanced respiration and primary productivity in warmer waters during baseflow (Rocher-Ros et al., 2021). For this reason, investigating GHG patterns with both seasonal and daily resolution is needed to rigorously quantify the fluxes at the annual scale. Thus, it has been shown that ignoring night-time emissions from humic lakes of western Siberia may strongly underestimate the summer-time CO_2 fluxes (i.e., Shirokova et al., 2020); however, it remains unknown, to which degree this is true for the rivers of the region.

Fourth, we hypothesized a direct control of land cover (bog, peatland, forest, riparian zone coverage) of the river watershed on GHG pattern in the river waters, as it is known for large Siberian rivers such as Lena (Vorobyev et al., 2021) and generally across the subarctic zone (Hutchins et al., 2019). Testing the above-stated factors to elucidate GHG emissions from the river water surfaces constituted the first objective of the present. Our second objective was to compare total C emission flux with lateral export (yield) of dissolved and particulate carbon of the rivers, and placing this finding within previous studies of Siberian rivers. The C emission: export ratio is a fundamental parameter of carbon biogeochemical cycle in riverine systems, which is needed for integral assessment of the role of lothic waters in C transport between the land and the sea (Serikova et al., 2018) and which allows discerning the degree to which terrestrial C is lost in the fluvial network or exported to downstream coastal areas (Striegl et al., 2012). Overall, we anticipate that results of the present work should allow better understanding of environmental controllers for CO_2 and CH_4 emissions from small Siberian rivers and may allow foreseeing future changes in fluvial exchange and export under on-going climate warming. This will constitute an important step towards large scale

modeling of C emission and export fluxes from permafrost-free forest and peatland rivers of the boreal zone.

2. Study site, materials and methods

2.1. Small and medium size WSL rivers

We studied 11 tributaries (watershed area from 0.8 to 5854 km^2, Fig. 1, Table S1) of the two largest eastern rivers draining to the Ob River: the Chulym and the Ket River (catchment areas of 134,000 and 94,000 km^2, respectively). The Strahler order of the studied rivers ranges from 1 to 9. Among these 11 rivers, two were not sampled during summer and autumn due to insufficient water level. The mean annual air temperature (MAAT) ranges from +0.1 °C at the Chulym watershed to −0.9 °C at the Ket watershed, and the mean annual precipitation is 520 ± 20 mm in this part of the WSL. The lithology of studied catchments is dominated by Pleistocene silts and sands with carbonate concretions overlayed by Quaternary loesses, fluvial, glacial and lacustrine deposits. The dominant soils are podzols in forest areas and histosols in peat bog regions. There is no permafrost on small rivers, but two large rivers (Ket and Chulym) exhibit between 5 and 14 % of isolated permafrost coverage. The chosen watersheds are highly contrasting in terms of land cover parameters (Table S1 of the Supplement). The peatland coverage ranges from 0 to 30 %, the dominant light needleleaf and broadleaf forest occupy from 1 to 70 %, and the grassland coverage varies from 0 to 19 %. There is no arable land of any agricultural use on studied rivers except Chulym (9.4 %).

The peak of annual discharge in WSL rivers of the permafrost-free zone occurs in the end of May; in August, the discharge is 3 to 5 times smaller (Pokrovsky et al., 2020). The seasonally frozen soil (0–30 cm) starts to thaw in the end of April – beginning of May and freezes in the beginning of October. During three main hydrological seasons in 2020, we visited 11 rivers from May 17 to 20, and 9 rivers from July 23 to 26 and from September 22 to 25. At about 500 m upstream of the river bridge, we collected surface water samples from the middle of the river (using waders or a boat depending on river depth) for determination of water characteristics and installed floating flux chambers as outlined below.

2.2. GHG concentrations and CO_2 fluxes by floating chambers

Surface water CO_2 concentration was measured in-situ at 0.3–0.5 m depth by submersing a portable infrared gas analyzer (IRGA, GMT222 CARBOCAP® probe, Vaisala®; accuracy ± 1.5 %) of two ranges (2000 and 10,000 ppm). A Campbell logger was connected to the system allowing continuous recording of the CO_2 concentration, water temperature and pressure every minute during at least 30 min of deployment.

In-situ CO_2 fluxes (FCO_2) were measured using floating chamber method. Typically, 3 to 4 replicate chambers were deployed at each river for a duration of 0.5 to 1.0 h. The chambers were small lightweight plastic bins (~30–32 cm in diameter, ~300 g, 10 L) equipped with non-dispersive infrared CO_2 loggers (SenseAir) (Bastviken et al., 2015). The CO_2 concentration inside the chamber was recorded continuously at 10 s interval and we used the first 10 to 30 min of measurements for computing CO_2 fluxes (Serikova et al., 2019). The CO_2 concentrations vs time were fit using a linear regression; in 99 % cases R^2 was higher than 0.80.

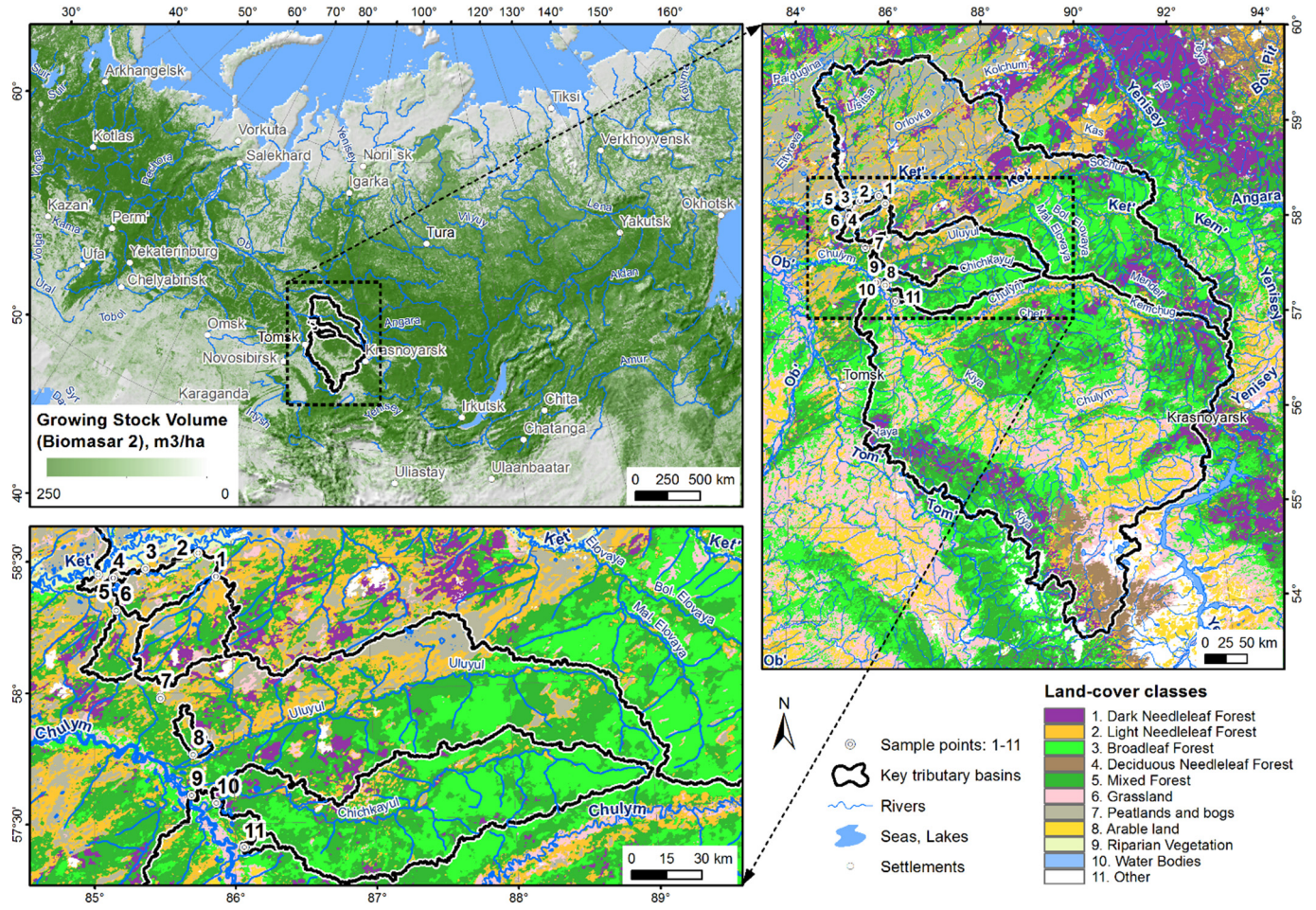

Fig. 1. Map of the sampling points and main land cover of the 11 river tributaries of the two main watersheds – Ket and Chulym. See parameters of the rivers in Table S1 of the Supplement.

Based on measured FCO_2 and CO_2 concentration in the river water, we obtained the gas transfer coefficient K_T using Fick's law (Eq. (1)):

$$FCO_2 = K_H \times K_T\ (C_{water} - C_{air}) \quad (1)$$

where K_H is the Henry's constant corrected for temperature and pressure (mol L^{-1} atm^{-1}) which also incorporates pH-dependent chemical enhancement factor, C_{water} is the water CO_2 concentration (ppmv), and C_{air} is the CO_2 concentration in the ambient air (ppmv).

For CH_4 analyses of grab samples, unfiltered water was collected from 30 cm depth in 60-mL Serum bottles, closed without air bubbles using vinyl stoppers and aluminum caps and immediately poisoned by adding 0.2 mL of saturated $HgCl_2$ via a two-way needle system. The samples were wrapped in aluminum foil and stored approximately one week in the refrigerator before the analyses. In the laboratory, a headspace was created by displacing approximately 40 % of water with N_2 (99.999 %). The delay between the sampling and the headspace creation never exceeded 1 week. In our previous methodological works in this region with DOC-rich surface waters, we verified that on-site and post-field laboratory headspace creation in the vials poisoned with $HgCl_2$ do not produce significantly different results (Shirokova et al., 2013; Pokrovsky et al., 2013). Two 0.5-mL replicates of the equilibrated headspace were analyzed for their concentrations of CH_4, using a Bruker GC-456 gas chromatograph (GC) equipped with flame ionization and thermal conductivity detectors (Serikova et al., 2019; Vorobyev et al., 2021). After every 10 samples, a calibration of the detectors was performed using Air Liquid gas standards (i.e. 145 ppmv). Duplicate injection of the samples showed that results were reproducible within ±5 %. The specific gas solubility for CH_4 (Yamamoto et al., 1976) were used in calculation of the CH_4 content in the water.

We calculated instantaneous diffusive CH_4 fluxes for each of the chambers using chamber-specific gas transfer velocity (K_T) and the concentrations of dissolved CH_4 in the water and in air-water equilibrium (atm = 1.8 ppm), following the procedure outlined in Serikova et al. (2018), who used the same setup for measurements of GHG emissions from rivers and lakes of the WSL. Note that this setup does not allow measuring the ebullitive CH_4 fluxes and thus it is possible that the evasion of CH_4, especially in the stagnant zone of the river flow and floodplain in this study is sizably underestimated (i.e., Stanley et al., 2016; Krickov et al., 2021; Villa et al., 2021).

2.3. Chemical analyses of river water

The dissolved oxygen (CellOx 325; accuracy of ±5 %), specific conductivity (TetraCon 325; ±1.5 %), and water temperature (±0.2 °C) were measured in-situ at 20 cm depth using a WTW 3320 Multimeter. The pH was measured using portable Hanna instrument via combined Schott glass electrode calibrated with NIST buffer solutions (4.01, 6.86 and 9.18 at 25 °C), with an uncertainty of 0.01 pH units. The temperature of buffer solutions was within ±5 °C of that of the river water. The water was sampled in pre-cleaned polypropylene bottle from 20 to 30 cm depth in the middle of the river and immediately filtered through disposable single-use sterile Sartorius filter units (0.45 μm pore size). The first 50 mL of filtrate was discarded. The DOC and Dissolved Inorganic Carbon (DIC) were determined by a Shimadzu TOC-VSCN Analyzer (Kyoto, Japan) with an uncertainty of 3 % and a detection limit of 0.1 mg L^{-1}. Blanks of Milli-Q water passed through the filters demonstrated negligible release of DOC from the filter material. For calculating $SUVA_{254}$, an indicator of aromaticity of DOM and its allochthonous (terrestrial) origin, we measured ultraviolet absorbance at 254 nm (UV_{254}) using a 10-mm quartz cuvette on a Bruker CARY-50 UV-VIS spectrophotometer.

The nutrient analyses were based on colorimetric assays (Koroleff, 1983a,b). Total dissolved organic nitrogen (DON) was measured from the difference between the total dissolved nitrogen (persulfate oxidation) and the total dissolved inorganic nitrogen (DIN, or the sum of NH_4^+, NO_2^- and NO_3^-). Uncertainties of DON and DIN analyses were between 10 and 20 % and detections limits were between 10 and 50 μg L^{-1}. The P-PO_4 analyses were based on the formation of molybdenum blue complex from the reaction of orthophosphate and ammonium molybdate followed by reduction with ascorbic acid in the aqueous sulfuric acid medium, with an uncertainty of 5 % and a detection limit of 2 μg L^{-1}.

The concentrations of C and N in total suspended solids (TSS) were determined via filtration of freshly collected river water (1–2 L) on-site (at the river bank or in the boat) with pre-weighted GFF filters (47 mm, 0.45 μm) and Nalgene 250-mL polystyrene filtration units using a Mityvac® manual vacuum pump. The C and N concentrations in the TSS (C_{TSS} and N_{TSS}, respectively) were measured using catalytic combustion with Cu-O at 900 °C with an uncertainty of ≤0.5 % using Thermo Flash 2000 CN Analyzer at EcoLab, Toulouse. The samples were analyzed before and after 1:1 HCl treatment to distinguish between total and inorganic C; however the ratio of $C_{organic}$: $C_{carbonate}$ in TSS was always above 20 and the contribution of carbonate C to total C in the TSS was equal in average 0.3 ± 0.3 % (2 s.d., n = 30). The TSS was examined by Scanning Electron Microscopy (SEM) using a JEOL JSM 6360LV SEM coupled with a SDD PGT Sahara EDS analyzer operating at 30 kV.

Total bacterial cell concentration (TBC) was measured after sample fixation in glutaraldehyde, by a flow cytometry (Guava® EasyCyte™ systems, Merck). Cells were stained using 1 μL of a 10 times diluted SYBR GREEN solution (10,000×, Merck), added to 250 μL of each sample before analysis. Particles were identified as cells based on green fluorescence and forward scatter (Marie et al., 1999).

2.4. Landscape parameters and water surface coverage of this part of the permafrost-free WSL territory

The physio-geographical characteristics of the Chulym and Ket Rivers and their selected tributaries were determined by applying available digital elevation model (DEM GMTED2010), soil, vegetation and lithological maps. The landscape parameters were typified using TerraNorte Database of Land Cover of Russia (Bartalev et al., 2011, http://terranorte.iki.rssi.ru). This included various types of forest (evergreen, deciduous, needle-leaf/broadleaf), grassland, tundra, wetlands, water bodies and other area. The climate the watershed were obtained from CRU grids data (1950–2016) (Harris et al., 2014) and NCSCD data (doi:https://doi.org/10.5879/ecds/00000001, Hugelius et al., 2013), respectively, whereas the biomass and soil OC content were obtained from BIOMASAR2 (Santoro et al., 2010) and NCSCD databases. The lithology layer was taken from GIS version of Geological map of the Russian Federation (scale 1: 5,000,000, http://www.geolkarta.ru/). We quantified river water surface area using the global SDG database with 30 m^2 resolution (Pekel et al., 2016) including both seasonal and permanent water for the open water period of 2020 and for the multiannual average (reference period 2000–2004). We also used a more recent GRWL Mask Database which incorporates first order wetted streams (Allen and Pavelsky, 2018).

GHG concentrations and fluxes and solute concentrations for all dataset were tested for normality using a Shapiro-Wilk test. Because data were not normally distributed, we used non-parametric statistics. Thus, the median and interquartile range (IQR) were used to represent C concentration and fluxes in sampled rivers. Comparisons of GHG concentration and CO_2 fluxes during different seasons were conducted using a non-parametric Mann Whitney test at a significance level of 0.05. For comparison of unpaired data, a non-parametric H-criterion Kruskal-Wallis test was used to reveal the differences between different study sites. The Pearson rank order correlation coefficient (Rs, $p < 0.05$) was used to determine the relationship between CO_2 concentrations and emission fluxes and main landscape parameters of the river watersheds, as well as other potential drivers such as DIC, DOC, POC and total bacterial number.

Table 1
Mean (±1SD) physical, chemical and biological characteristics of the water column for the 11 small and middle size WSL rivers.

Parameter	Spring	Summer	Autumn	All season
pCO_2, μatm	6300 ± 2320	4450 ± 3640	4010 ± 4540	5010 ± 3580
CH_4, μmol L^{-1}	1.47 ± 1.33	3.31 ± 5.17	5.65 ± 8.56	3.25 ± 5.53
N_{RSM}, mg g^{-1}	10.2 ± 4.31	8.79 ± 3.2	12.6 ± 6.38	10.5 ± 4.85
C_{RSM}, mg g^{-1}	140 ± 73.4	126 ± 63.9	158 ± 72	142 ± 68.8
K_T, m d^{-1}	0.954 ± 0.316	1.91 ± 1.28	1.45 ± 1.09	1.40 ± 1.00
FCO_2, g C m^{-2} d^{-1}	2.92 ± 1.81	1.72 ± 0.913	2.38 ± 4.26	2.40 ± 2.57
FCH_4, mmol m^{-2} d^{-1}	5.67 ± 6.1	34.6 ± 74.2	43.1 ± 72.1	25.7 ± 57.2
POC, mg L^{-1}	1.37 ± 1.08	1.37 ± 0.713	1.29 ± 1.04	1.35 ± 0.935
DIC, mg L^{-1}	2.57 ± 2.88	19.1 ± 13.8	20.7 ± 16	13.3 ± 14.3
DOC, mg L^{-1}	28.4 ± 8.18	11 ± 3.67	9.93 ± 4.68	17.3 ± 10.6
$SUVA_{254}$	4.4 ± 0.37	3.55 ± 0.474	3.35 ± 0.653	3.81 ± 0.679
Cl, mg L^{-1}	0.193 ± 0.154	0.323 ± 0.33	0.46 ± 0.557	0.316 ± 0.375
SO_4, mg L^{-1}	1.38 ± 1.74	1.46 ± 2.38	1.87 ± 3.36	1.56 ± 2.44
P_{total}, μg L^{-1}	44 ± 10.8	44.1 ± 11.5	35.2 ± 10.3	41.3 ± 11.3
N_{total}, μg L^{-1}	847 ± 146	489 ± 99.1	489 ± 89	625 ± 210
TBC, cells mL^{-1}	$1.0 \times 10^7 \pm 7.3 \times 10^6$	$1.7 \times 10^6 \pm 1.1 \times 10^6$	$3.7 \times 10^6 \pm 2.9 \times 10^6$	$5.6 \times 10^6 \pm 3.0 \times 10^6$

3. Results

3.1. Seasonal variations of particulate and dissolved carbon in river water

The concentration of suspended material in studied rivers varied from 1.1 to 27 mg L^{-1} without systematic effect of seasons (Table 1, Fig. 2 A). Particulate Organic Carbon (POC) concentration ranged from 0.2 to 4.5 mg C L^{-1} with maximal variations observed during the spring flood and minimal variations observed during autumn baseflow (Fig. 2 B). The content of organic carbon in the TSS ranged from 13 % in spring and summer to 20.5 % in the autumn baseflow. High C_{org} content in the TSS was further confirmed by SEM and elementary study of the suspended matter on filters collected from small rivers, especially during spring flood (Fig. S2 A, B). In large rivers (Chulym and Ket), the TSS was represented by mineral components such as quartz and feldspars with sizable amount of diatom frustules and phytoliths (Fig. S2 C–F). The total bacterial number was the highest during spring flood and the lowest during autumn baseflow (Table 1).

The DOC and DIC concentration in small rivers were subjected to strong seasonal variations, with almost 3-fold decrease in DOC concentration from the spring to the autumn, and a 7 to 8-fold increase in DIC concentration between spring and summer-autumn (Fig. 2 C, D). This pattern was observed for both second and third order streams, but also two large rivers (Ket and Chulym). The SUVA remained quite stable across seasons with 20–25 % higher values during spring flood compared to summer and autumn baseflow. The nutrient concentrations were more conservative across seasons compared to that of C, especially for phosphorus (P_{tot}, P-PO_4), while

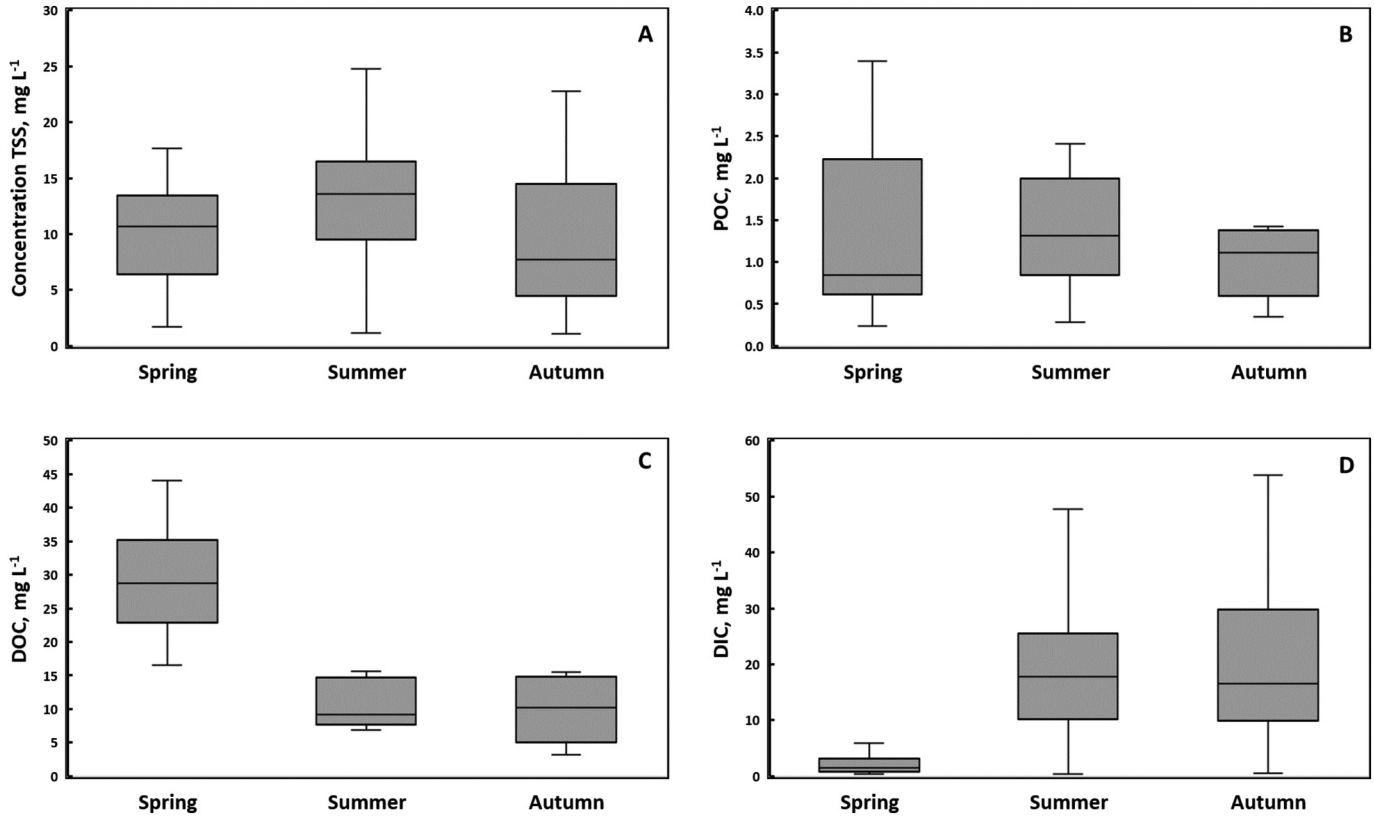

Fig. 2. Concentration of total river suspended matter (**A**), particulate organic carbon (**B**), DOC (**C**) and DIC (**D**) in small and medium-size rivers of WSL across seasons (median and IQR).

for nitrogen there were a two-fold increase in [NH_4] and a two-fold decrease in [N_{tot}] between spring and summer-autumn (Table 1).

3.2. GHG regime: seasonal and diel variations

CO_2 concentrations were highest ($p < 0.05$) during season of spring flood (6300 ppm) and decreased approximately 1.5 times during summer and autumn (Fig. 3 A). CH_4 concentrations and fluxes increased in the order spring ≤ summer < autumn and ranged from 1 to 15 μmol L^{-1} and from 5 to 100 mmol m^{-2} d^{-1}, respectively (Fig. 3 B, D). The emissions of CO_2 decreased ($p < 0.05$) from spring to summer and autumn, from 2.9 ± 1.8 to 2.0 ± 0.3 g C m^{-2} d^{-1}, respectively (Fig. 3 C). These values are consistent to CO_2 emissions reported by Serikova et al. (2018) for other rivers of the WSL permafrost-free zone.

The diel variations of CO_2 concentration and emissions were assessed for two small rivers, Inguzet and Suiga ($S_{watershed}$ of 1216 and 464 km^2, respectively) during all three hydrological seasons (Fig. 4). The difference in CO_2 emission fluxes between day and night was not significant (Mann-Whitney *U* test difference, $p > 0.05$), and the FCO_2 varied within <10–20 %. The diel variations of pCO_2 and FCO_2 were not related to those of temperature, pH and O_2 (not shown).

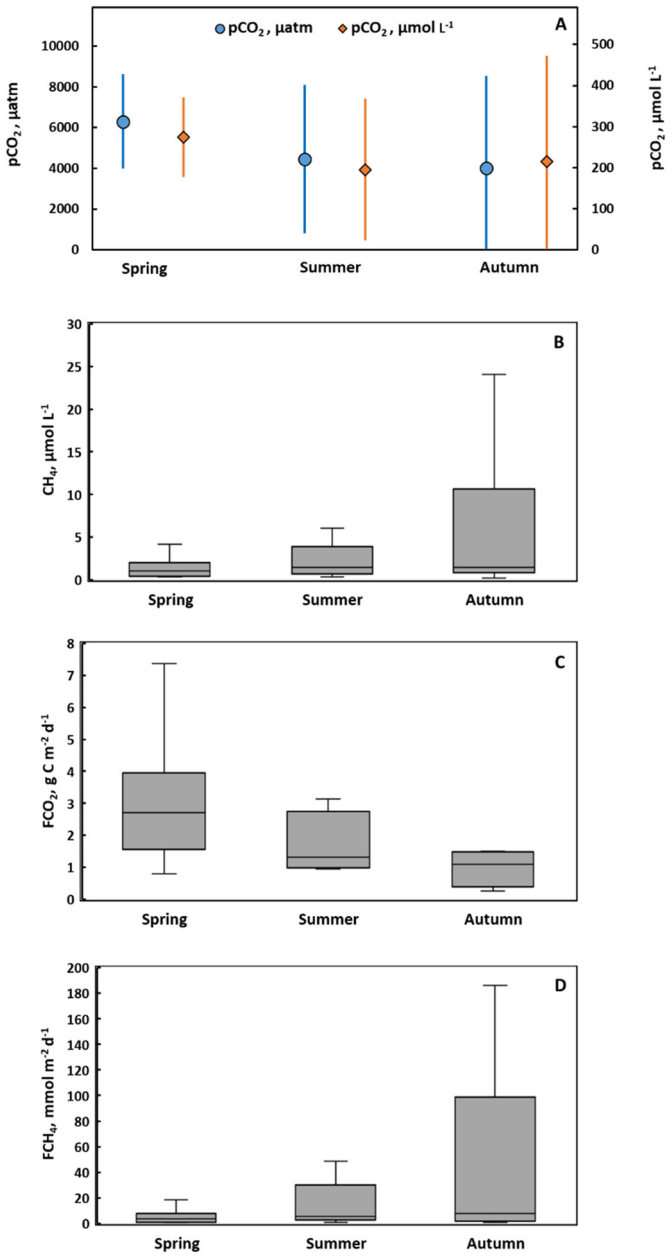

Fig. 3. Median (IQR, range) concentrations of CO_2 (**A**) and CH_4 (**B**) and fluxes of CO_2 (**C**) and CH_4 (**D**) in rivers of the WSL during three main hydrological seasons.

3.3. Potential controlling factors of C concentration and emission

The CO_2 concentration in the river water decreased with the size of the watershed during summer and autumn but less so in spring (Fig. 5 A; Table 2). However, the watershed size exerted negligible impact on measured CO_2 emission and CH_4 concentration and calculated CH_4 emissions regardless of seasons (Fig. 5 B, C). Among other hydrochemical parameters, only DIC and organic C concentration in the TSS sizably increased with the catchment size, whereas DOC, POC, TBC, and nutrient concentration did not exhibit any link with $S_{watershed}$ (Fig. S3).

The CO_2 and CH_4 concentrations positively correlated with DOC and POC, major nutrients and bacteria (Figs. S4 and S5 of the Supplement). However, these correlations were strongly season-specific (Table 2). Thus, in spring, CO_2 concentration significantly ($p < 0.05$) correlated with C and N content in the TSS, in summer it correlated only with dissolved NH_4, and for all seasons the correlations of CO_2 were significant with POC, P_{tot} and NH_4. Methane concentration was significantly ($p < 0.05$) correlated with C_{TSS}, DOC, NO_3 and TBC in spring; PO_4 in summer, and dissolved and particulate N in autumn.

The impact of the water column physico-chemical and biological parameters on the CO_2 fluxes was also variable among seasons. Thus, FCO_2 significantly ($p < 0.05$) correlated to NO_2 concentration and TBC in spring; TBC in summer and POC in autumn (Table 2). When considering all seasons together, FCO_2 were positively correlated to the sum of concentrations of particulate and dissolved organic carbon (R^2 = 0.3–0.5, $p < 0.05$, Fig. S6), total dissolved N and P, and TBC (Fig. 6).

Among the landscape parameters, only the proportion of light needle-leaf forest and wetlands at the watershed positively correlated with CO_2 fluxes in spring (Fig. 7 A, B; Table 3). These land cover parameters also correlated with CO_2 concentrations (Fig. 7 C, D) although these correlations were generally weaker than those with riparian zone coverage; the latter was also correlated with both CO_2 and CH_4 concentrations during summer and autumn (Fig. 7 E, F; Table 3). Note however that these dependences could partially reflect an artifact due to lack of data points between 20 and 95 % of riparian coverage of the river watershed. Furthermore, the resolution of land cover for 1st and 2nd order streams could not allow quantifying direct impact of some landscape type on GHG pattern in the river water.

3.4. Carbon emission and export from WSL river watersheds

Considering that 3 main hydrological seasons allow first-order assessment of C (>99.5 % CO_2, <0.5 % CH_4) evasion from river surfaces, we calculated the average land-area normalized riverine evasion flux for 6 open water months as the sum of spring (May and June), summer (July and August) and autumn (September and October). The seasonal and permanent river water surface areas (lakes excluded) provided by GIS assessment for the Ket River and Chylum River basins (to which the sampled rivers belong) for 6 months of open water period were 427 and 1007 km^2, respectively. The main rationale of using GIS-based total river water surface area for calculating areal C emissions is that the watershed area and stream order did not exert significant impact on FCO_2 and FCH_4 (see Section 3.3).

The measured 6-month average C emission for both river basins (2.40 g C-CO_2 m^{-2} d^{-1}, Table 1) multiplied by total river water surface area yields a C evasion of 2.1×10^{11} and 5.0×10^{11} g C yr^{-1} for Ket and Chulym basins. These values were normalized to the surface area of Ket and Chulym basins sampled in this work (67,141 and 119,117 km^2 land area, respectively) thus yielding net evasion of 3.6 t C km^{-2} over 6 month period. This value contain major uncertainties, likely at least 30 %, related to the spatial and seasonal variations in measured CO_2 emission fluxes and poorly constrained seasonal water coverage, given sizable floodplain of both rivers in this part of the WSL.

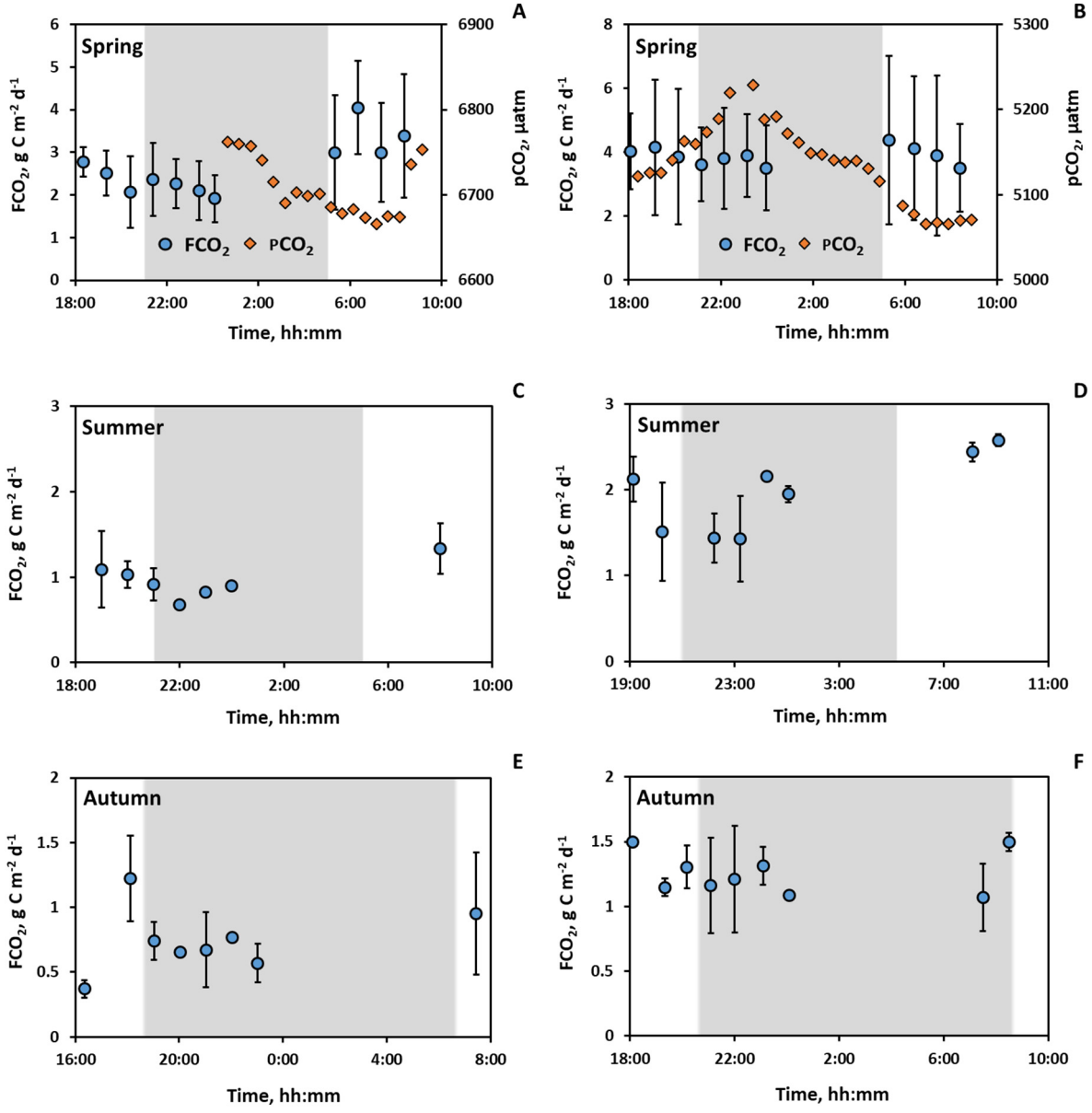

Fig. 4. Diel variations of CO_2 concentrations (A, B) and CO_2 emissions (A–F) of two small rivers of the WSL (Inguzet, $S_{watershed}$ = 1216 km^2, A, C, E and Suiga, $S_{watershed}$ = 464 km^2, B, D, F) during spring flood and summer and autumn baseflow.

The lateral yield of C by western Siberian rivers is fairly well constrained by studies of particulate (Krickov et al., 2018) and dissolved (Pokrovsky et al., 2020) organic and inorganic C fluxes measured with sufficient seasonal and spatial resolution. According to these studies, over 6 months of open water period, from May to October, small and medium-size rivers in the southern (permafrost-free) part of the WSL export 1.2 t DOC km^{-2}, 2.1 t DIC km^{-2}, and 0.1 t POC km^{-2}. Therefore, the total dissolved + particulate C export (3.4 t km^{-2}/period) of small and medium size southern WSL rivers is similar to total CO_2 evasion from the river surfaces during the same open-water period of the year.

4. Discussion

4.1. Potential drivers of aquatic C (POC, DOC, DIC) concentration in small WSL rivers

The average concentrations of TSS in studied WSL rivers (10–13 mg L^{-1}) are in general agreement with those of other small and medium-size boreal rivers of low runoff, draining through wetland territories (Krickov et al., 2018, 2020). The concentrations of POC in studied river waters were similar to the values measured to other small and medium size rivers of the WSL obtained by our group (Krickov et al., 2020) and other researchers (1.2–2.4 mg L^{-1}, Gebhardt et al., 2005; Le Fouest et al., 2013; McClelland et al., 2016). These values are generally consistent with mean annual POC of subarctic Eurasian river that drain through wetland territories such as Severnaya Dvina, Pechora, and Ob (Gordeev et al., 1996; Pokrovsky et al., 2010; Savenko et al., 2004). Note quite high concentration of organic C in the TSS observed in the WSL rivers (13 to 20 %). This is much higher than the world river average of 1 % (Meybeck, 1993) and the concentrations reported in the Ob, Lena, Yenisey and Kolyma Rivers (2.3, 3.6, 5.0 and 3.0 %, respectively, Gordeev and Kravchishina, 2009). For example, typical POC concentration in the TSS of large ($S_{watershed}$ > 100,000 km^2) rivers of Central Siberia are between 0.4 and 0.5 % (Pokrovsky et al., 2005), and in the Severnaya Dvina River that has sizable amount of wetlands on its watershed, the C_{org} concentration in the TSS is between 2 and 6 % (Savenko et al., 2004). In small rivers of the WSL, sizable amount of the TSS is represented by peat and vegetation debris, especially during spring flood. Indeed, the main source of OM in these rivers is

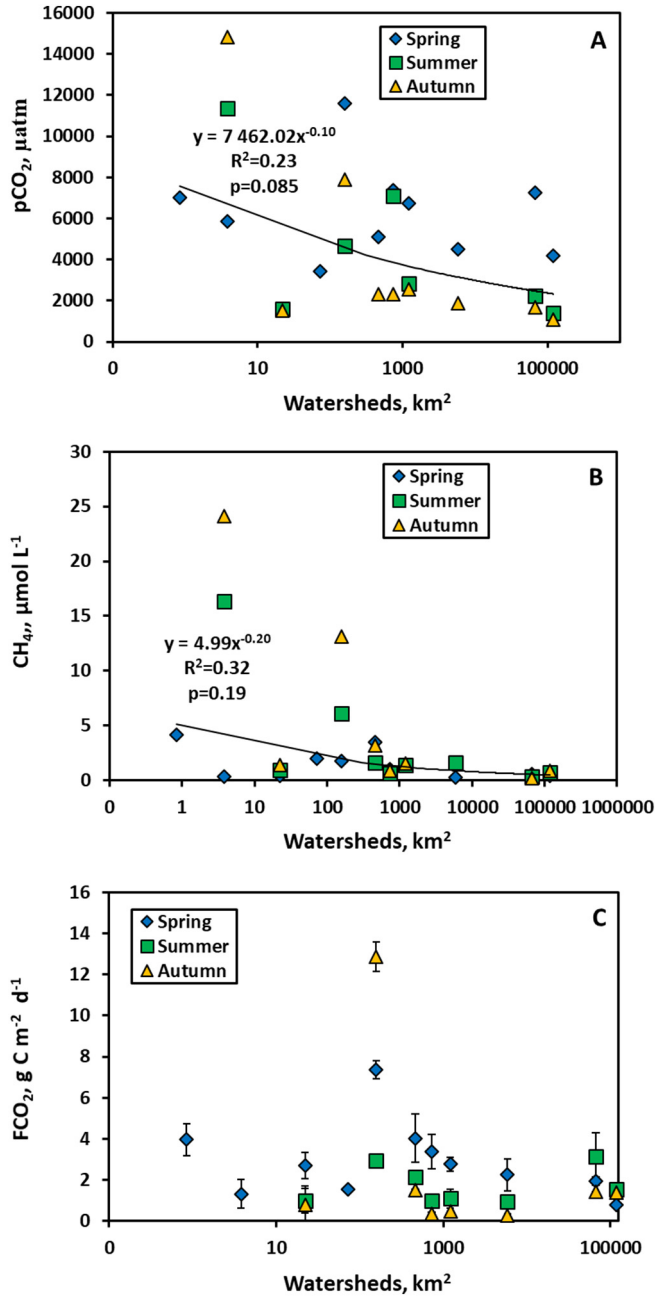

Fig. 5. Weak dependences of CO_2 (A) and CH_4 (B) concentrations and lack of CO_2 emission dependence (C) on river watershed area of small and medium size WSL rivers during three seasons. The regression line fits the data of all seasons together.

organic-rich waterlogged riparian soils, along with plant litter that is delivered to the river from large floodplains especially during the spring freshet. During summer and autumn baseflow, the TSS contains large amount of phytoplankton debris which is likely due to increase in biological productivity with water temperature. Such high concentration of organic carbon in the riverine particulate material likely promote strong heterotrophic degradation and provide necessary niches for OM-mineralizing bacteria (Attermeyer et al., 2018).

The DOC concentration of studied WSL rivers (10 to 30 mg L^{-1}) is consistent with former results of our group (Pokrovsky et al., 2015; Pokrovsky et al., 2020) and other researchers (Frey and Smith, 2005) on other rivers of the WSL region in particular and peatland catchments of the boreal zone in general (Hope et al., 1994, 2001; Dinsmore et al., 2013; Dyson et al., 2011). Similar to POC, DOC concentration exhibited a maximum during spring flood period, as also reported for the Ob River middle course ($S_{watershed}$ = 260,000 km^2) of the region (Vorobyev et al., 2019). The spring maximum of DOC concentration can be linked to strong leaching of DOC from plant litter at the flood zone, as it is known for other riverine systems (i.e., Greenway et al., 2006). Another source of elevated DOC during this period of the year could be DOC mobilization from peatlands, due to high hydrological connectivity between these organic-rich mires and rivers (Ala-aho et al., 2018). As such, high DOC concentrations in small WSL rivers corroborate numerous former studies of other regions (i.e., Mzobe et al., 2020), which demonstrate that catchments with low runoff and high proportion of mires exhibit the highest DOC concentrations (Kicklighter et al., 2013) and that small size catchments (headwaters) have higher DOC concentrations due to higher connectivity between terrestrial DOC sources and adjacent streams (Ågren et al., 2007).

The seasonal pattern of DIC concentration was opposite to that of DOC, with a maximum during baseflow and a minimum during the spring flood. This is consistent with DIC control by the underground discharge from carbonate mineral-bearing sedimentary deposits, as it is known for other riverine systems of the WSL permafrost-free zone (Pokrovsky et al., 2020), including the largest one, the Ob River in its middle course (Vorobyev et al., 2019). Furthermore, progressive involvement of soil mineral layers in DIC mobilization from spring to summer and autumn may produce gradual enrichment in DIC in shallow (subsurface) flow that feeds the river.

4.2. Physico-chemical and microbiological parameters impacting the GHG regime

Despite significant progress in quantifying the patterns of C evasion from lotic waters over past two decades (Butman and Raymond, 2011; Duvert et al., 2018; Hotchkiss et al., 2015; Horgby et al., 2019; Schneider et al., 2020; Gómez-Gener et al., 2021a,b; Hao et al., 2021; M. Li et al., 2021; Y. Li et al., 2021; Xiao et al., 2021; Liu et al., 2022), regional estimates of CO_2 emissions in rivers and streams are highly variable, due mostly to strong heterogeneity of water objects and insufficient knowledge of factors controlling the emissions (Richey et al., 2002; Humborg et al., 2010; Striegl et al., 2012; Borges et al., 2015; Pearce et al., 2022). One of such factor can be particulate organic matter supplied to river and streams via soil and shore erosion, given that the rate of POC biodegradation greatly (more than an order of magnitude) exceeds that of DOC (Attermeyer et al., 2018). The permafrost-free rivers studied in the present work are strongly enriched in organic matter which is supplied from the watershed via shallow subsurface and surface runoff, mostly from coastal peatlands erosion and floodplain drainage. Elevated concentrations of organic carbon in the TSS of studied rivers may be linked to weak erosional force of the streamflow, given low river slope (typically from 0.2 to 0.7 m km^{-1}) and limited involvement of minerals into particle transport. It is thus possible that high CO_2 emissions from rivers of this region are due to efficient bioprocessing of elevated amount of particulate organic matter in the water column. Most likely, microbial activity in suspended solids, leading to efficient POC biodegradation (i.e., Attermeyer et al., 2018), largely contributed to GHG emissions. Results of the present study are consistent with this hypothesis because both the concentration and emission of CO_2 and CH_4 concentration positively correlated with riverine POC across the seasons (Table 2; Fig. 6A). The overwhelming role of OM biodegradation in CO_2 emission is further confirmed by a positive relationship between FCO_2 and total bacteria count (Fig. 6 E).

The CO_2 fluxes also exhibited positive (although not significant at $p < 0.05$) correlations with DOC of the water column. The DOC has been reported as important driver of dissolved CO_2 in surface waters (Lennon, 2004; Xiao et al., 2020). Therefore, the first hypothesis of the present study – an overwhelming role of POC and DOC mineralization as driver for CO_2 emission – is found to be consistent with obtained results, as confirmed by positive ($R_{Pearson}$ = 0.60–0.68, $p < 0.05$) correlations of FCO_2 with sum of DOC and POC concentrations. We suggest that high concentrations of organic matter in river water, notably in most headwater streams, allow efficient mineralization processes thus producing the highest CO_2 concentrations (Fig. 5 A). This possibility is consistent with other studies across the world (M. Li et al., 2021; Y. Li et al., 2021), including boreal

Table 2
Linear (Pearson) correlation matrix of GHG and C concentrations and CO_2 fluxes with the main characteristics of the water column. TSS is for total suspended solids. Significance: * $p < 0.05$.

	Spring			Summer			Autumn			All season		
	FCO_2	$[CO_2]$	$[CH_4]$	FCO_2	$[CO_2]$	$[CH_4]$	FCO_2	$[CO_2]$	$[CH_4]$	FCO_2	$[CO_2]$	$[CH_4]$
n	*11*	*10*	*11*	*8*	*7*	*9*	*8*	*9*	*8*	*27*	*26*	*28*
$SUVA_{254}$	0.31	0.15	0.60	0.43	−0.21	−0.02	−0.16	−0.32	−0.49	0.11	0.08	−0.35
O_2	−0.49	−0.83*	0.10	−0.11	−0.96*	−0.84*	−0.17	−0.57	−0.52	−0.01	−0.33	0.07
pH	−0.09	−0.11	−0.35	0.12	0.28	0.11	−0.06	0.01	0.09	−0.14	−0.14	0.17
T_{water}	0.03	0.30	−0.08	−0.09	−0.84*	−0.68*	−0.29	−0.67*	−0.62	−0.10	−0.12	−0.48*
TSS	0.09	−0.16	0.09	0.25	0.21	0.14	0.85*	0.65	0.66	0.41*	0.30	0.31
N_{TSS}	0.61*	0.75*	0.32	0.12	0.11	0.15	−0.08	−0.34	−0.32	0.13	−0.03	−0.06
C_{TSS}	0.68*	0.67*	0.62*	−0.18	−0.03	0.02	−0.01	−0.30	−0.29	0.18	0.02	−0.03
POC	0.62*	0.47	0.34	0.31	0.64	0.37	0.94*	0.47	0.47	0.70*	0.48*	0.33
DIC	−0.03	0.02	−0.31	−0.22	0.2	0	−0.11	−0.04	0.16	−0.18	−0.17	0.20
DOC	0.63*	0.35	0.86*	0.63	−0.32	−0.08	0.44	−0.28	−0.38	0.37	0.23	−0.24
C total	0.67*	0.39	0.85*	0.68	−0.2	−0.01	0.60	−0.16	−0.25	0.42*	0.27	−0.21
Cl	−0.45	−0.55	−0.29	−0.06	−0.35	−0.21	0	−0.22	−0.2	−0.08	−0.34	−0.09
SO_4	−0.55	−0.70*	−0.28	−0.12	−0.38	−0.21	−0.18	−0.28	−0.25	−0.23	−0.37	−0.19
PO_4	−0.13	−0.28	−0.05	0.59	0.74	0.77*	−0.29	−0.42	−0.41	−0.01	0.26	0.04
P total	0.06	−0.04	−0.02	0.33	0.61	0.62	−0.19	0.52	0.44	0	0.48*	0.25
NO_2	0.72*	0.55	0.75*	0.41	0.45	0.45	−0.01	−0.34	−0.48	0.30	0.34	−0.18
NO_3	0.37	0.10	0.86*	−0.24	0.6	0.43	−0.01	−0.34	−0.50	0.16	0	−0.03
NH_4	−0.44	−0.11	−0.55	0.01	0.76*	0.44	−0.23	0.71*	0.64	−0.20	0.47*	0.55*
N total	0.53	0.32	0.44	0.61	0.32	0.40	0.38	−0.22	−0.29	0.34	0.30	−0.19
TBC	0.81*	0.56	0.66*	0.85*	0.45	0.41	0.57	−0.02	−0.06	0.51*	0.35	−0.06

non-permafrost regions (Hotchkiss et al., 2015; Marx et al., 2017) and specifically, small-scale peatland settings (Dawson et al., 2001, 2004; Leith et al., 2014, 2015).

The second hypothesis of this study – on the watershed size and OM quality control on GHG emissions – could not been verified neither for individual seasons, nor for the full open-water period of observations. Although the pCO_2 decreased with $S_{watershed}$ increase during all three season, the FCO_2 remained independent on the watershed size and stream order, and Pearson correlations were not significant ($p > 0.05$, see Tables 2 and 3). As for the DOM quality, which is reflected by SUVA, there was no link between this parameter and riverine GHG concentration and fluxes. It is possible that relatively high and stable $SUVA_{254}$ across the river size and season (3.8 ± 0.7 L mg C^{-1} m^{-1}) corresponds to stable input of essentially allochthonous DOM from surrounding peatlands which does not vary across the river size and period of the year.

The lack of diel cycle in CO_2 emission over all three contrasting seasons (no difference in FCO_2 between the day and night, see Fig. 4) suggests a negligible role of both photo-degradation of OM and primary production in the rivers, including both the water column (plankton) and the river bed (periphyton). This result dismisses the third hypothesis of this study, that the diurnal variations in C emissions are mostly pronounced during summer/autumn baseflow.

4.3. Landscape control on C emissions from river waters

Examining the land cover control on C concentrations and emissions allowed testing the fourth hypothesis of this study. The CO_2 flux from the river surface to the atmosphere during the spring flood was sizably higher than that during baseflow, suggesting, in accord with observations in other small streams of wetlands (i.e., Khadka et al., 2014) that excess precipitation (or snow thaw) flushes soil organic carbon to the river via surface and shallow subsurface flow. At the same time, this finding contrasts the results of studies in other boreal catchments, where elevated CO_2 during summer compared to other seasons was due to enhanced microbial respiration, DOM photodegradation and groundwater import at low flow conditions (D'Amario and Xenopoulos, 2015), as also known from coastal peatlands (Dinsmore et al., 2010). We believe that the primary source of the springtime elevated CO_2 in WSL river waters could be wetlands and bogs, as consistent with *i*) positive correlations between this type of land cover and both pCO_2 and FCO_2 during spring (Fig. 7 B, D) and *ii*) strongest connectivity between wetlands and rivers during this period of the year as demonstrated by water isotope study in the permafrost-free WSL streams (Ala-aho et al., 2018). In this regard, homogeneous land coverage by peatland and taiga forest of studied watersheds provides stable allochthonous input of DOM as confirmed by weak spatial and seasonal variations of DOM aromaticity. These factors may be partially responsible for relatively weak impact of the land cover on CO_2 and CH_4 emissions measured in this study.

At the same time, the riparian zones and floodplain of even small rivers of the WSL may turn out to be the main sites of elevated CO_2 generation in the water column as supported by a positive correlation ($R_{Pearson}$ = 0.81–0.84, $p < 0.01$) between pCO_2 and riparian vegetation of the watershed during summer and autumn baseflow (Table 3, Fig. 7 F). Specifically, a positive control of ammonia and phosphate on both CO_2 and CH_4 concentration in the summer likely reflects respiration of sediments accompanied by enhanced diffusion of these nutrients from partially anoxic pore waters to the water column. The latter is consistent with anoxic environment at the bottom layers of flooded zones and a negative correlation of both GHG with O_2 concentration in the water column during summer and spring. Similar features were reported for the middle course of the Ob River (i.e., Krickov et al., 2021) and agricultural river network of subtropical climate (Xiao et al., 2021) whereas numerous observations in other boreal regions demonstrated that the lateral transfer of CO_2 from the terrestrial to the aquatic system is strongly controlled by the riparian zones (Leith et al., 2015; Ledesma et al., 2018; Abril and Borges, 2019). In Ontario streams, Canada, elevated CO_2 concentrations were linked to terrestrially-derived DOM, originated from riparian wetlands, where CO_2 was imported with this complex material and produced through microbial respiration (D'Amario and Xenopoulos, 2015).

Among other land cover drivers of CO_2 emissions during high water season is the presence of light needle-leaf forest which positively correlated with pCO_2 and FCO_2 (Fig. 7 A, C). This type of trees could supply elevated amount of POC (in the form of needle litter) during spring flood at high flow when massive mobilization of the vegetation debris from the forest floor to the river occurs. As discussed above, this fresh particular organic matter, in turn, could enhance the CO_2 production in the water column.

The pattern of CH_4 concentration dependence on hydrochemical parameters of the water column and land cover of the river watershed was generally similar to that of CO_2, with strong impact of POC, DOC, dissolved N and bacteria concentration in spring, dissolved P and N in summer and particulate and dissolved N in autumn (Table 2). This pattern could reflect methane generation within local hot spots associated with organic-rich particles of the water column. Among the landscape parameters of the

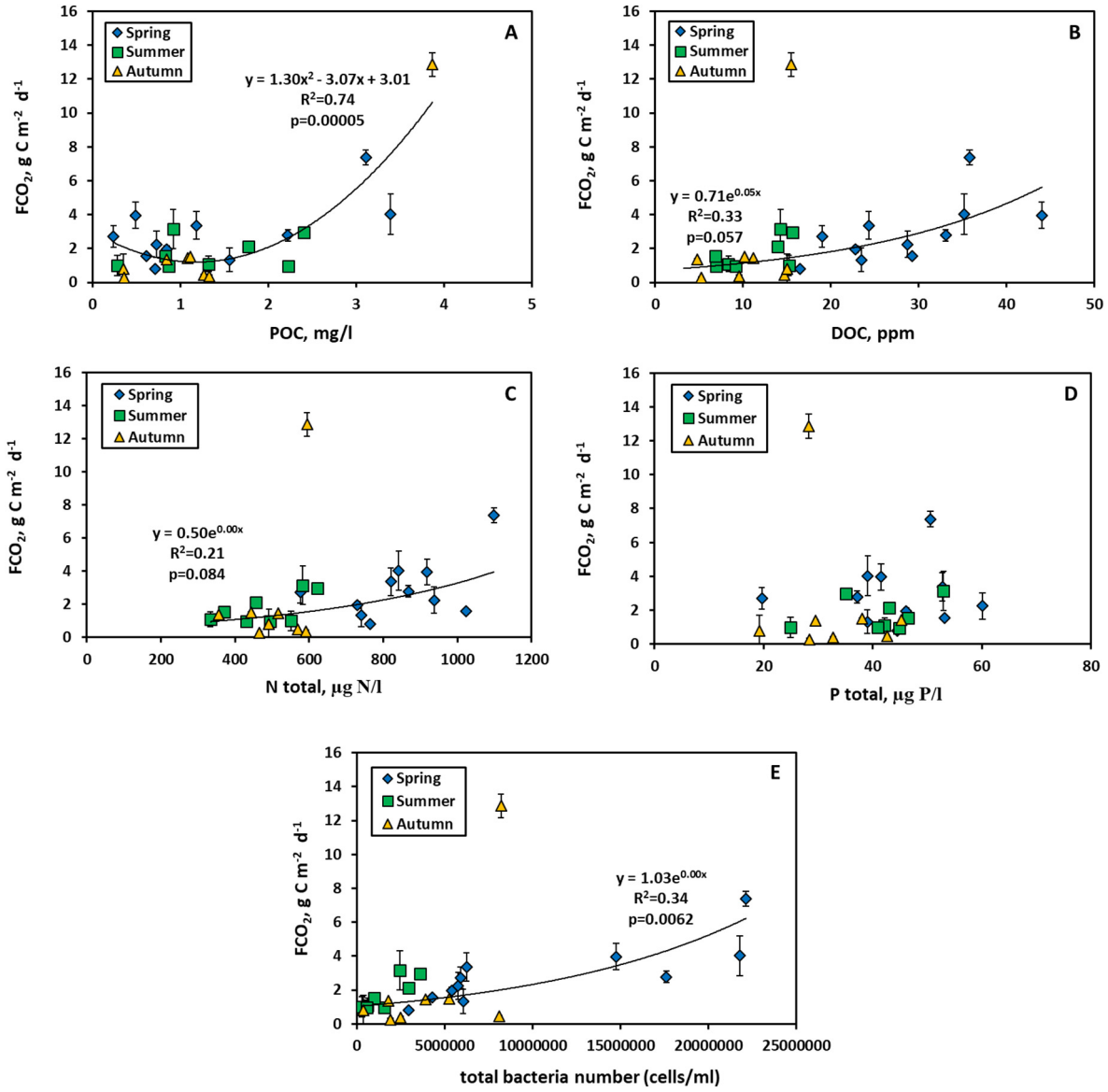

Fig. 6. CO_2 flux dependence on particulate (A) and dissolved (B) organic carbon, dissolved nitrogen (C) and phosphorus (D) and total bacterial number (E). The regression line fits the data of all three seasons together. Only significant ($R_{Pearson} > 0.40$, $p < 0.05$) correlations are shown.

watershed, only the coverage by riparian vegetation positively correlated with CH_4 concentration during summer and autumn (Table 3, Fig. 7 E) which is consistent with CH_4 generation in nutrient-rich sediments of the floodplain or stagnant zones of the river bed and its riparian zone. Therefore, the fourth hypothesis of the present study – about strong land cover control on GHG emissions – was only partially verified by obtained data since, among the landscape parameters, only riparian zone vegetation correlated with CH_4 concentrations in the river water, but none of the land cover parameters impacted the CO_2 flux.

4.4. Carbon emission and export

The areal normalized C emission fluxes (CO_2, >99.5 %; CH_4, <0.5 %) during 6 months of open water period in the rivers belonging to Ket and Chulym watersheds range from 3 to 4 t C km^{-2} y^{-1}, respectively, which is comparable to the dissolved (DOC + DIC) and particulate C yield of WSL rivers at this latitude (3.4 ± 0.4 t C km^{-2} y^{-1}). These values are in agreement with emission: export ratio close to 1 reported by Serikova et al. (2018) for other WSL permafrost-free rivers (essentially eastern tributaries of the Ob River in its middle course, not belonging to the Ket and Chulym watersheds). Moreover, the ratio assessed in the present work across three seasons is consistent with the value of 1.3:1 for global inland waters (Raymond et al., 2013; Lauerwald et al., 2015). Altogether, this shows the significance to account for riverine C emissions in order to understand the fate of terrestrial C and its link to the large hydrological C cycle. Overall, the fate of terrestrial C export may be sensitive to changes in climate and terrestrial C cycling and runoff. In the present study, we suggest that the fluxes are largely driven by riverine mineralization of terrestrial OC in the water column (both DOC and POC), coupled with respiration at the river bottom and riparian sediments. Thus, raised temperature may facilitate larger internal losses therefore increasing the ratio of evasion to export. In contrast, increased runoff and lower transit times of water due to enhanced precipitation, notably during summer and autumn, could result in the opposite trend. This dual effect of on-going climate change on aquatic C cycling is a particular feature of boreal zone with humic rivers capable to process terrestrial OC and which would not have been the case if emissions are largely driven by CO_2 supply from land (Vachon et al., 2021).

Furthermore, given that the vegetation of the riparian zone was the sole environmental parameter significantly ($p < 0.05$) and positively correlated with CO_2 and CH_4 concentrations (Table 3), we strengthen the importance

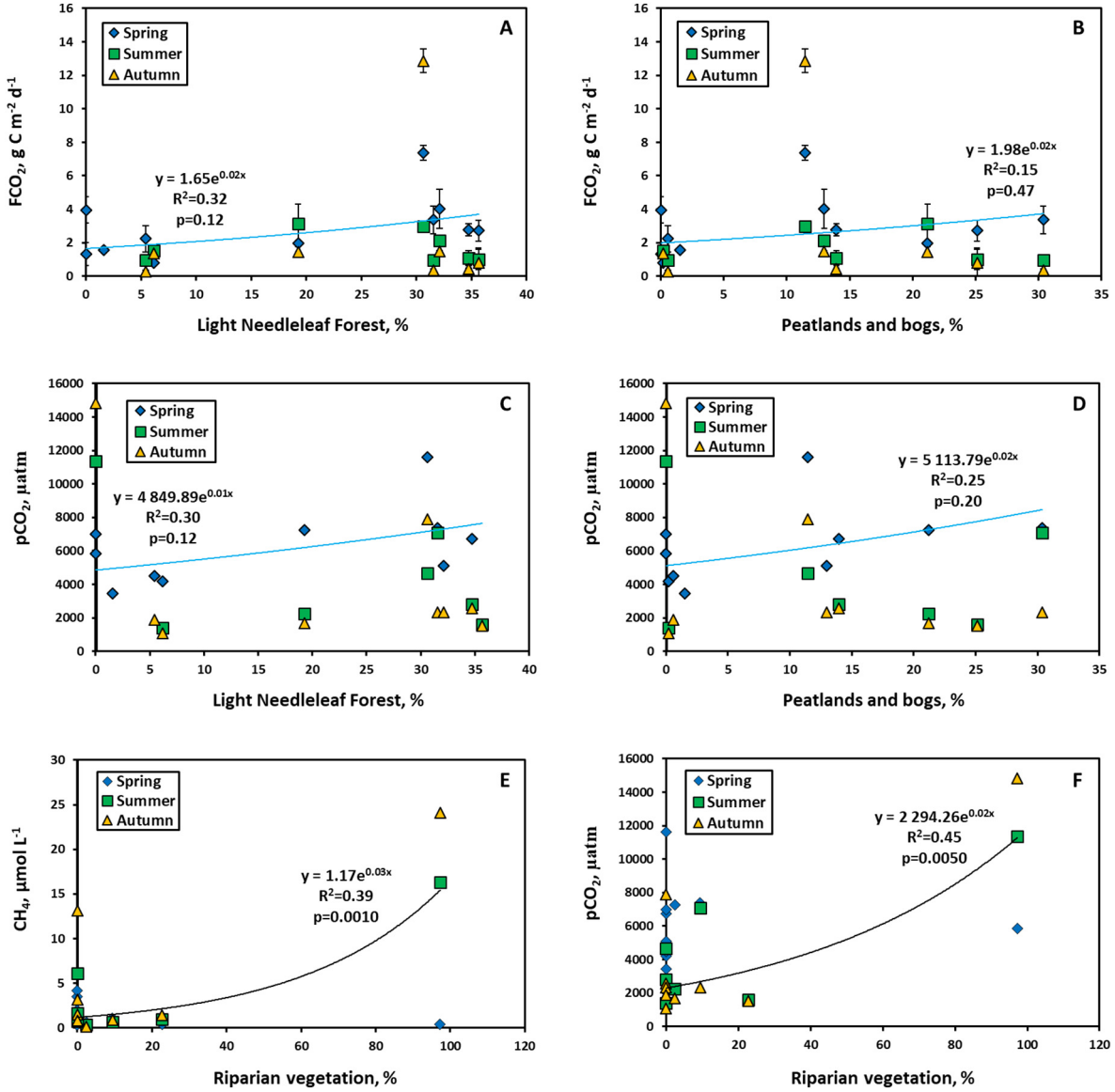

Fig. 7. Positive correlations of CO_2 fluxes (A, B) and CO_2 and CH_4 concentrations (C–F) with landscape parameters of the watersheds across seasons. The regression line on A to D fits the data during spring period, when the links are strongly pronounced, but the fit to the data on CO_2 and CH_4 dependence on riparian vegetation is for summer and autumn.

of the changes in the hydrological regime of the river floodplain and riparian vegetation productivity for assessing the response of GHG pattern in the river waters to the climate change in this part of Siberia. On a global scale, current C emissions from inland waters of the whole WSL reach nearly half (35–50 %) of the region's land C uptake (Karlsson et al., 2021). The effect of C emission from water surfaces can be even more important in the northern, permafrost-affected part of the WSL territory, given that the lakes can strongly offset net terrestrial C uptake by tundra vegetation (Beckebanze et al., 2022). In this regard, on-going increase in terrestrial biomass and greening of the tundra biome (Berner et al., 2020) can sizably modify the C balance between the land and the atmosphere via decreasing the share of C fluvial emissions.

5. Conclusions

A combined GHG emission and dissolved and particulate carbon dynamics in 11 small and medium size western Siberian rivers in the permafrost-free zone during three main hydrological seasons allowed quantification of C fluxes and testing the main physico-chemical, and biological factors of the water column and watershed landscape characteristics controlling the C export and evasion. The particulate and dissolved organic carbon revealed strong correlations with CO_2 emissions and thus could be responsible for sizable CO_2 generation in the water column and/or concomitant export from the peatland and forest zones of the watersheds. The latter mechanism is supported by a sizable increase in CO_2 concentration with a decrease of watershed size during summer and autumn baseflow suggesting CO_2 generation in some hotspots of the peatland and riparian zones hydrologically connected to the smallest rivers. This is consistent with the result that, among various physico-chemical and biological parameters of the water column, DOC, POC, total bacterial cells and nutrients exhibited positive correlation with CO_2 and CH_4 concentrations and CO_2 fluxes. The underground discharge of carbonate-rich waters, mostly pronounced during summer and autumn did not sizably contribute to CO_2 evasion from the rivers. Instead, the CO_2 and CH_4 pattern in the river was most likely controlled by a combination of continuous input of C-rich peatland waters and diffusion from riparian sediments and flooded vegetation and in-stream processes (OC mineralization).

Table 3
Linear (Pearson) correlation matrix of GHG and C concentrations and CO_2 fluxes with the main watershed parameters of small and medium size WSL rivers. Significance: * $p < 0.05$.

	n	Area watershed	Dark Needleleaf Forest	Light Needleleaf Forest	Deciduous Forest	Mixed Forest	Grassland	Peatlands and bogs	Arable land	Riparian Vegetation	Water Bodies	Biomass
Spring												
CO_2	*10*	−0.23	0.22	0.52	−0.23	−0.22	−0.13	0.44	−0.32	−0.05	−0.08	−0.15
CH_4	*11*	−0.36	−0.02	−0.02	0.33	0.42	−0.45	−0.19	−0.26	−0.35	−0.37	0.47
FCO_2	*11*	−0.45	0.14	0.49	−0.13	0.18	−0.25	0.24	−0.39	−0.3	−0.28	0.22
POC	*11*	−0.27	0.55	0.5	−0.52	0.17	−0.34	0.09	−0.2	−0.03	−0.26	0.27
DIC	*11*	0.70*	0.24	−0.2	0.06	0.13	0.57	−0.37	0.84*	−0.2	0.43	0.13
DOC	*11*	−0.56	0.04	−0.02	0.38	0.46	−0.67*	−0.26	−0.48	−0.31	−0.55	0.62*
N_{TSS}	*11*	−0.51	−0.17	0.11	−0.12	−0.05	−0.39	0.09	−0.46	0.23	−0.25	0.06
C_{TSS}	*11*	−0.54	−0.08	0.19	0.12	−0.07	−0.37	0.06	−0.45	0.01	−0.41	0.06
Summer												
CO_2	*7*	−0.49	−0.53	−0.41	−0.46	−0.35	−0.6	−0.23	−0.37	0.81*	−0.11	0.04
CH_4	*9*	−0.29	−0.44	−0.48	−0.28	−0.36	−0.35	−0.48	−0.19	0.89*	−0.38	0.05
FCO_2	*8*	0.24	0.45	0.02	−0.15	0.36	−0.29	−0.01	−0.08	−0.39	−0.15	0.37
POC	*9*	−0.4	0.07	0.19	−0.47	0.3	−0.52	0.07	−0.29	0.1	0.05	0.36
DIC	*9*	0.31	−0.08	−0.74*	0.89*	0.32	−0.08	−0.6	0.32	−0.08	0.33	0.43
DOC	*9*	−0.23	0.06	0.46	−0.32	0.17	−0.11	0.32	−0.42	−0.17	−0.54	0.1
N_{TSS}	*9*	−0.75*	−0.23	0.66	−0.64	0.02	−0.19	0.44	−0.65	0.04	−0.54	−0.03
C_{TSS}	*9*	−0.71*	−0.3	0.73*	−0.67*	−0.19	0.04	0.51	−0.55	0.06	−0.53	−0.29
Autumn												
CO_2	*9*	−0.34	−0.4	−0.39	−0.35	−0.3	−0.39	−0.4	−0.24	0.84*	−0.38	0.08
CH_4	*8*	−0.35	−0.45	−0.52	−0.35	−0.22	−0.4	−0.57	−0.23	0.81*	−0.44	0.22
FCO_2	*8*	−0.15	0.07	0.19	−0.29	0.44	−0.11	−0.13	−0.1	−0.24	−0.28	0.43
POC	*9*	−0.21	0.18	0.23	−0.42	0.35	−0.25	−0.01	−0.16	−0.03	−0.17	0.4
DIC	*9*	0.38	−0.08	−0.79*	0.91*	0.35	−0.03	−0.68*	0.39	−0.08	0.27	0.47
DOC	*9*	−0.35	0.34	0.90*	−0.54	0.15	0.03	0.65	−0.41	−0.45	−0.33	−0.09
N_{TSS}	*9*	−0.37	−0.24	0.59	−0.26	−0.24	0.27	0.52	−0.38	−0.15	−0.42	−0.41
C_{TSS}	*9*	−0.51	−0.2	0.67*	−0.32	−0.14	0.15	0.55	−0.49	−0.18	−0.48	−0.32
All seasons												
CO_2	*26*	−0.34	−0.27	−0.19	−0.19	−0.17	−0.41*	−0.18	−0.29	0.54*	−0.22	0.09
CH_4	*28*	−0.25	−0.28	−0.29	−0.19	−0.18	−0.29	−0.34	−0.17	0.61*	−0.32	0.09
FCO_2	*27*	−0.18	0.08	0.19	−0.15	0.27	−0.17	−0.02	−0.16	−0.15	−0.24	0.31
POC	*29*	−0.28	0.31	0.33	−0.47*	0.25	−0.35	0.05	−0.21	0.001	−0.16	0.33
DIC	*29*	0.3	0.04	−0.39*	0.38*	0.11	0.05	−0.36	0.31	−0.04	0.26	0.2
DOC	*29*	−0.26	−0.04	0.04	0.17	0.3	−0.25	−0.04	−0.26	−0.2	−0.3	0.29
N_{TSS}	*29*	−0.46*	−0.19	0.39*	−0.24	−0.1	−0.05	0.32	−0.42*	0.02	−0.35	−0.14
C_{TSS}	*29*	−0.57*	−0.17	0.47*	−0.18	−0.12	−0.08	0.33	−0.48*	−0.04	−0.46*	−0.15

The C emission (>99.5 % CO_2; <0.5 % CH_4) to export (DOC, DIC, POC) ratio of permafrost-free WSL rivers was close to 1 and consistent with the world average. Among land cover parameters, only the riparian vegetation was positively correlated with CO_2 and CH_4 concentrations in the river water. As such, under climate warmings scenario, the change in the hydrological regime of the floodplain and riparian vegetation productivity likely to be the main factors controlling the response of GHG pattern in the river water.

CRediT authorship contribution statement

IK and OP designed the study and wrote the paper; IK, AL performed sampling, analysis and their interpretation; MK performed landscape characterization of the watersheds and calculated water surface area; LS performed bacterial number assessment and DOC results interpretation; JK provided analyses of literature data, transfer coefficients for FCO_2 calculations and global estimations of areal emission vs export.

Data availability

Pokrovsky, Oleg; Lim, Artyom; Крицков, Иван; Korets, Mikhail (2022), "C concentrations and CO2 fluxes in western Siberian rivers", Mendeley Data, v1 http://dx.doi.org/10.17632/twftb6ffdj.1.

Declaration of competing interest

The authors declare that they have no conflict of interest.

Acknowledgements

We acknowledge funding from RFBR grant 20-05-00729 and grant "Kolmogorov" of MES (Agreement No 075-15-2022-241). The work was also supported by the TSU Program Priority-2030.

Appendix A. Supplementary data

Supplementary data to this article can be found online at https://doi.org/10.1016/j.scitotenv.2022.160202.

References

Abril, G., Borges, A.V., 2019. Ideas and perspectives: carbon leaks from flooded land: do we need to replumb the inland water active pipe? Biogeosciences 16, 769–784. https://doi.org/10.5194/bg-16-769-2019.

Ågren, A., Buffam, I., Jansson, M., Laudon, H., 2007. Importance of seasonality and small streams for the landscape regulation of dissolved organic carbon export. J. Geophys. Res. Biogeosci. 112. https://doi.org/10.1029/2006JG000381.

Ala-aho, P., Soulsby, C., Pokrovsky, O.S., Kirpotin, S.N., Karlsson, J., Serikova, S., Vorobyev, S.N., Manasypov, R.M., Loiko, S., Tetzlaff, D., 2018. Using stable isotopes to assess surface water source dynamics and hydrological connectivity in a high-latitude wetland and permafrost influenced landscape. J. Hydrol. 556, 279–293. https://doi.org/10.1016/j.jhydrol.2017.11.024.

Allen, G.H., Pavelsky, T.M., 2018. Global extent of rivers and streams. Science 361, 585–588. https://doi.org/10.1126/science.aat0636.

Attermeyer, K., Catalán, N., Einarsdottir, K., Freixa, A., Groeneveld, M., Hawkes, J.A., Bergquist, J., Tranvik, L.J., 2018. Organic carbon processing during transport through boreal inland waters: particles as important sites. J. Geophys. Res. Biogeosci. 123, 2412–2428. https://doi.org/10.1029/2018JG004500.

Bartalev, S.A., Egorov, V.A., Ershov, D.V., Isaev, A.S., Lupyan, E.A., Plotnikov, D.E., Uvarov, I.A., 2011. Remote mapping of vegetation land cover of Russia based on data of MODIS spectroradmeter. Mod. Probl. Earth Remote Sens. Space 8, 285–302.

Bastviken, D., Sundgren, I., Natchimuthu, S., Reyier, H., Gålfalk, M., 2015. Technical note: cost-efficient approaches to measure carbon dioxide (CO_2) fluxes and concentrations in terrestrial and aquatic environments using mini loggers. Biogeosciences 12, 3849–3859. https://doi.org/10.5194/bg-12-3849-2015.

Battin, T.J., Luyssaert, S., Kaplan, L.A., Aufdenkampe, A.K., Richter, A., Tranvik, L.J., 2009. The boundless carbon cycle. Nat. Geosci. 2, 598–600. https://doi.org/10.1038/ngeo618.

Beckebanze, L., Rehder, Z., Holl, D., Wille, C., Mirbach, C., Kutzbach, L., 2022. Ignoring carbon emissions from thermokarst ponds results in overestimation of tundra net carbon uptake. Biogeosciences 19, 1225–1244. https://doi.org/10.5194/bg-19-1225-2022.

Berner, L.T., Massey, R., Jantz, P., Forbes, B.C., Macias-Fauria, M., Myers-Smith, I., Kumpula, T., Gauthier, G., Andreu-Hayles, L., Gaglioti, B.V., Burns, P., Zetterberg, P., D'Arrigo, R., Goetz, S.J., 2020. Summer warming explains widespread but not uniform greening in the Arctic tundra biome. Nat. Comm. 11, 4621. https://doi.org/10.1038/s41467-020-18479-5.

Borges, A.V., Darchambeau, F., Teodoru, C.R., Marwick, T.R., Tamooh, F., Geeraert, N., Omengo, F.O., Guérin, F., Lambert, T., Morana, C., Okuku, E., Bouillon, S., 2015. Globally significant greenhouse-gas emissions from African inland waters. Nat. Geosci. 8, 637–642. https://doi.org/10.1038/ngeo2486.

Bretz, K.A., Jackson, A.R., Rahman, S., Monroe, J.M., Hotchkiss, E.R., 2021. Integrating ecosystem patch contributions to stream corridor carbon dioxide and methane fluxes. J. Geophys. ResBiogeosciences 126, e2021JG006313. https://doi.org/10.1029/2021JG006313.

Bring, A., Fedorova, I., Dibike, Y., Hinzman, L., Mård, J., Mernild, S.H., Prowse, T., Semenova, O., Stuefer, S.L., Woo, M.-K., 2016. Arctic terrestrial hydrology: a synthesis of processes, regional effects, and research challenges. J. Geophys. Res. Biogeosci. 121, 621–649. https://doi.org/10.1002/2015JG003131.

Butman, D., Raymond, P.A., 2011. Significant efflux of carbon dioxide from streams and rivers in the United States. Nat. Geoscience 4 (10), 1–4. https://doi.org/10.1038/ngeo1294.

Campeau, A., del Giorgio, P.A., 2014. Patterns in CH_4 and CO_2 concentrations across boreal rivers: major drivers and implications for fluvial greenhouse emissions under climate change scenarios. Glob. Chang. Biol. 20, 1075–1088. https://doi.org/10.1111/gcb.12479.

Campeau, A., Lapierre, J.-F., Vachon, D., del Giorgio, P.A., 2014. Regional contribution of CO_2 and CH_4 fluxes from the fluvial network in a lowland boreal landscape of Québec. Glob. Biogeochem. Cycl. 28, 57–69. https://doi.org/10.1002/2013GB004685.

Castro-Morales, K., Canning, A., Körtzinger, A., Göckede, M., Küsel, K., Overholt, W.A., Wichard, T., Redlich, S., Arzberger, S., Kolle, O., Zimov, N., 2022. Effects of reversal of water flow in an Arctic floodplain river on fluvial emissions of CO_2 and CH_4. J. Geophys. Res. Biogeosciences 127, e2021JG006485. https://doi.org/10.1029/2021JG006485.

Chadburn, S.E., Krinner, G., Porada, P., Bartsch, A., Beer, C., Belelli Marchesini, L., Boike, J., Ekici, A., Elberling, B., Friborg, T., Hugelius, G., Johansson, M., Kuhry, P., Kutzbach, L., Langer, M., Lund, M., Parmentier, F.-J.W., Peng, S., Van Huissteden, K., Wang, T., Westermann, S., Zhu, D., Burke, E.J., 2017. Carbon stocks and fluxes in the high latitudes: using site-level data to evaluate earth system models. Biogeosciences 14, 5143–5169. https://doi.org/10.5194/bg-14-5143-2017.

Chen, L., Aalto, J., Luoto, M., 2021. Significant shallow–depth soil warming over Russia during the past 40 years. Glob. Planet. Change 197, 103394. https://doi.org/10.1016/j.gloplacha.2020.103394.

Crawford, J.T., Striegl, R.G., Wickland, K.P., Dornblaser, M.M., Stanley, E.H., 2013. Emissions of carbon dioxide and methane from a headwater stream network of interior Alaska. J. Geophys. Res. Biogeosci. 118, 482–494. https://doi.org/10.1002/jgrg.20034.

D'Amario, S.C., Xenopoulos, M.A., 2015. Linking dissolved carbon dioxide to dissolved organic matter quality in streams. Biogeochemistry 126, 99–114. https://doi.org/10.1007/s10533-015-0143-y.

Dawson, J.J., Billett, M.F., Hope, D., Palmer, S.M., Deacon, C., 2004. Sources and sinks of aquatic carbon in a peatland stream continuum. Biogeochemistry 70, 71–92.

Dawson, J.J.C., Billett, M.F., Hope, D., 2001. Diurnal variations in the carbon chemistry of two acidic peatland streams in north-East Scotland. Freshw. Biol. 46, 1309–1322. https://doi.org/10.1046/j.1365-2427.2001.00751.x.

Denfeld, B.A., Frey, K.E., Sobczak, W.V., Mann, P.J., Holmes, R.M., 2013. Summer CO_2 evasion from streams and rivers in the Kolyma River basin, north-east Siberia. Polar Res. 32, 19704. https://doi.org/10.3402/polar.v32i0.19704.

Dinsmore, K.J., Billett, M.F., Moore, T.R., 2009. Transfer of carbon dioxide and methane through the soil-water-atmosphere system at Mer Bleue peatland, Canada. Hydrol. Process. 23, 330–341. https://doi.org/10.1002/hyp.7158.

Dinsmore, K.J., Billett, M.F., Skiba, U.M., Rees, R.M., Drewer, J., Helfter, C., 2010. Role of the aquatic pathway in the carbon and greenhouse gas budgets of a peatland catchment. Glob. Chang. Biol. 16, 2750–2762.

Dinsmore, K.J., Billett, M.F., Dyson, K.E., 2013. Temperature and precipitation drive temporal variability in aquatic carbon and GHG concentrations and fluxes in a peatland catchment. Glob. Change Biol. 19, 2133–2148. https://doi.org/10.1111/gcb.12209.

Duvert, C., Butman, D.E., Marx, A., Ribolzi, O., Hutley, L.B., 2018. CO_2 evasion along streams driven by groundwater inputs and geomorphic controls. Nat. Geosci. 11, 813–818. https://doi.org/10.1038/s41561-018-0245-y.

Dyson, K.E., Billett, M.F., Dinsmore, K.J., Harvey, F., Thomson, A.M., Piirainen, S., Kortelainen, P., 2011. Release of aquatic carbon from two peatland catchments in E. Finland during the spring snowmelt period. Biogeochemistry 103, 125–142. https://doi.org/10.1007/s10533-010-9452-3.

Frey, K.E., Smith, L.C., 2005. Amplified carbon release from vast west Siberian peatlands by 2100. Geophys. Res. Lett. 32, 1–4. https://doi.org/10.1029/2004GL022025.

Gebhardt, A.C., Gaye-Haake, B., Unger, D., Lahajnar, N., Ittekkot, V., 2005. A contemporary sediment and organic carbon budget for the Kara Sea shelf (Siberia). Mar. Geol. 220, 83–100. https://doi.org/10.1016/j.margeo.2005.06.035.

Gómez-Gener, L., Hotchkiss, E.R., Laudon, H., Sponseller, R.A., 2021a. Integrating dschargeconcentration dynamics across carbon forms in a boreal landscape. Water Resour. Res. 57, e2020WR028806. https://doi.org/10.1029/2020WR028806.

Gómez-Gener, L., Rocher-Ros, G., Battin, T., Cohen, M.J., Dalmagro, H.J., Dinsmore, K.J., Drake, T.W., Duvert, C., Enrich-Prast, A., Horgby, Å., Johnson, M.S., Kirk, L., Machado-Silva, F., Marzolf, N.S., McDowell, M.J., McDowell, W.H., Miettinen, H., Ojala, A.K., Peter, H., Pumpanen, J., Ran, L., Riveros-Iregui, D.A., Santos, I.R., Six, J., Stanley, E.H., Wallin, M.B., White, S.A., Sponseller, R.A., 2021b. Global carbon dioxide efflux from rivers enhanced by high nocturnal emissions. Nat. Geosci. 1–6. https://doi.org/10.1038/s41561-021-00722-3.

Gordeev, V., Martin, J., Sidorov, I., Sidorova, M., 1996. A reassessment of the Eurasian river input of water, sediment, major elements, and nutrients to the Arctic Ocean. Am. J. Sci. 296, 664–691. https://doi.org/10.2475/ajs.296.6.664.

Gordeev, V.V., Kravchishina, M.D., 2009. River flux of dissolved organic carbon (DOC) and particulate organic carbon (POC) to the Arctic Ocean: what are the consequences of the global changes? In: Nihoul, J.C.J., Kostianoy, A.G. (Eds.), Influence of Climate Change on the Changing Arctic and Sub-Arctic Conditions, NATO Science for Peace and Security Series C: Environmental Security. Springer Netherlands, Dordrecht, pp. 145–160 https://doi.org/10.1007/978-1-4020-9460-6_11

Greenway, H., Armstrong, W., Colmer, T.D., 2006. Conditions leading to high CO2 (>5 kPa) in waterlogged–flooded soils and possible effects on root growth and metabolism. Ann. Bot. 98, 9–32. https://doi.org/10.1093/aob/mcl076.

Hao, X., Ruihong, Y., Zhuangzhuang, Z., Zhen, Q., Xixi, L., Tingxi, L., Ruizhong, G., 2021. Greenhouse gas emissions from the water–air interface of a grassland river: a case study of the Xilin River. Sci. Rep. 11, 2659. https://doi.org/10.1038/s41598-021-81658-x.

Harris, I., Jones, P.D., Osborn, T.J., Lister, D.H., 2014. Updated high-resolution grids of monthly climatic observations – the CRU TS3.10 Dataset. Int. J. Climatol. 34, 623–642. https://doi.org/10.1002/joc.3711.

Hope, D., Billett, M.F., Cresser, M.S., 1994. A review of the export of carbon in river water: fluxes and processes. Environ. Pollut. 84, 301–324. https://doi.org/10.1016/0269-7491(94)90142-2.

Hope, D., Palmer, S.M., Billett, M.F., Dawson, J.J.C., 2001. Carbon dioxide and methane evasion from a temperate peatland stream. Limnol. Oceanogr. 46, 847–857. https://doi.org/10.4319/lo.2001.46.4.0847.

Horgby, Å., Segatto, P.L., Bertuzzo, E., Lauerwald, R., Lehner, B., Ulseth, A.J., Vennemann, T.W., Battin, T.J., 2019. Unexpected large evasion fluxes of carbon dioxide from turbulent streams draining the world's mountains. Nat. Commun. 10, 4888. https://doi.org/10.1038/s41467-019-12905-z.

Hotchkiss, E.R., Hall Jr., R.O., Sponseller, R.A., Butman, D., Klaminder, J., Laudon, H., Rosvall, M., Karlsson, J., 2015. Sources of and processes controlling CO_2 emissions change with the size of streams and rivers. Nat. Geosci. 8, 696–699. https://doi.org/10.1038/ngeo2507.

Hugelius, G., Tarnocai, C., Broll, G., Canadell, J.G., Kuhry, P., Swanson, D.K., 2013. The northern circumpolar soil carbon database: spatially distributed datasets of soil coverage and soil carbon storage in the northern permafrost regions. Earth Syst. Sci. Data 5, 3–13. https://doi.org/10.5194/essd-5-3-2013.

Humborg, C., Mörth, C.-M., Sundbom, M., Borg, H., Blenckner, T., Giesler, R., Ittekkot, V., 2010. CO_2 supersaturation along the aquatic conduit in swedish watersheds as constrained by terrestrial respiration, aquatic respiration and weathering. Glob. Change Biol. 16, 1966–1978. https://doi.org/10.1111/j.1365-2486.2009.02092.x.

Hutchins, R.H.S., Prairie, Y.T., del Giorgio, P.A., 2019. Large-scale landscape drivers of CO2, CH4, DOC, and DIC in boreal river networks. Glob. Biogeochem. Cycl. 33, 125–142. https://doi.org/10.1029/2018GB006106.

Karlsson, J., Serikova, S., Vorobyev, S.N., Rocher-Ros, G., Denfeld, B., Pokrovsky, O.S., 2021. Carbon emission from Western siberian inland waters. Nat. Commun. 12, 825. https://doi.org/10.1038/s41467-021-21054-1.

Khadka, M.B., Martin, J.B., Jin, J., 2014. Transport of dissolved carbon and CO2 degassing from a river system in a mixed silicate and carbonate catchment. J. Hydrol. 513, 391–402. https://doi.org/10.1016/j.jhydrol.2014.03.070.

Kicklighter, D.W., Hayes, D.J., McClelland, J.W., Peterson, B.J., McGuire, A.D., Melillo, J.M., 2013. Insights and issues with simulating terrestrial DOC loading of Arctic river networks. Ecol. Appl. 23, 1817–1836. https://doi.org/10.1890/11-1050.1.

Koprivnjak, J.-F., Dillon, P.J., Molot, L.A., 2010. Importance of CO2 evasion from small boreal streams. Glob. Biogeochem. Cycl. 24, GB4003. https://doi.org/10.1029/2009GB003723.

Koroleff, F., 1983a. Total and organic nitrogen. In: Grasshoff, K., Ehrhardt, M., Kremling, K. (Eds.), Methods for Seawater Analysis. Verlag Chemie, Weinheim, pp. 162–168.

Koroleff, F., 1983b. Determination of phosphorus. In: Grasshoff, K., Ehrhardt, M., Kremling, K. (Eds.), Methods for Seawater Analysis. Verlag Chemie, Weinheim, pp. 125–136.

Krickov, I.V., Lim, A.G., Manasypov, R.M., Loiko, S.V., Shirokova, L.S., Kirpotin, S.N., Karlsson, J., Pokrovsky, O.S., 2018. Riverine particulate C and N generated at the permafrost thaw front: case study of western Siberian rivers across a 1700 km latitudinal transect. Biogeosciences, 6867–6884 https://doi.org/10.5194/bg-15-6867-2018.

Krickov, I.V., Lim, A.G., Manasypov, R.M., Loiko, S.V., Vorobyev, S.N., Shevchenko, V.P., Dara, O.M., Gordeev, V.V., Pokrovsky, O.S., 2020. Major and trace elements in suspended matter of western siberian rivers: first assessment across permafrost zones and landscape parameters of watersheds. Geochim. Cosmochim. Acta 269, 429–450. https://doi.org/10.1016/j.gca.2019.11.005.

Krickov, I.V., Serikova, S., Pokrovsky, O.S., Vorobyev, S.N., Lim, A.G., Siewert, M.B., Karlsson, J., 2021. Sizable carbon emission from the floodplain of Ob River. Ecol. Indic. 131, 108164. https://doi.org/10.1016/j.ecolind.2021.108164.

Lauerwald, R., Laruelle, G.G., Hartmann, J., Ciais, P., Regnier, P.A.G., 2015. Spatial patterns in CO2 evasion from the global river network. Glob. Biogeochem. Cycl. 29, 534–554. https://doi.org/10.1002/2014GB004941.

Le Fouest, V., Babin, M., Tremblay, J.-É., 2013. The fate of riverine nutrients on Arctic shelves. Biogeosciences 10, 3661–3677. https://doi.org/10.5194/bg-10-3661-2013.

Ledesma, J.L.J., Futter, M.N., Blackburn, M., Lidman, F., Grabs, T., Sponseller, R.A., Laudon, H., Bishop, K.H., Köhler, S.J., 2018. Towards an improved conceptualization of riparian zones in boreal forest headwaters. Ecosystems 21, 297–315. https://doi.org/10.1007/s10021-017-0149-5.

Leith, F.I., Garnett, M.H., Dinsmore, K.J., Billett, M.F., Heal, K.V., 2014. Source and age of dissolved and gaseous carbon in a peatland–riparian–stream continuum: a dual isotope (14C and δ13C) analysis. Biogeochemistry 119, 415–433. https://doi.org/10.1007/s10533-014-9977-y.

Leith, F.I., Dinsmore, K.J., Wallin, M.B., Billett, M.F., Heal, K.V., Laudon, H., Öquist, M.G., Bishop, K., 2015. Carbon dioxide transport across the hillslope–riparian–stream continuum in a boreal headwater catchment. Biogeosciences 12, 1881–1892. https://doi.org/10.5194/bg-12-1881-2015.

Lennon, J.T., 2004. Experimental evidence that terrestrial carbon subsidies increase CO_2 flux from lake ecosystems. Oecologia 138, 584–591. https://doi.org/10.1007/s00442-003-1459-1.

Li, M., Peng, C., Zhang, K., Xu, L., Wang, J., Yang, Y., Li, P., Liu, Z., He, N., 2021. Headwater stream ecosystem: an important source of greenhouse gases to the atmosphere. Water Res. 190, 116738. https://doi.org/10.1016/j.watres.2020.116738.

Li, Y., Shang, J., Zhang, C., Zhang, W., Niu, L., Wang, L., Zhang, H., 2021. The role of freshwater eutrophication in greenhouse gas emissions: a review. Sci. Total Environ. 768, 144582. https://doi.org/10.1016/j.scitotenv.2020.144582.

Lim, A.G., Krickov, I.V., Vorobyev, S.N., Korets, M.A., Kopysov, S.G., Shirokova, L.S., Karlsson, J., Pokrovsky, O.S., 2022. Carbon emission and export from Ket River, western Siberia. EGUsphere Prepr. https://doi.org/10.5194/egusphere-2022-485.

Liu, S., Kuhn, C., Amatulli, G., Aho, K., Butman, D.E., Allen, G.H., Lin, P., Pan, M., Yamazaki, D., Brinkerhoff, C., Gleason, C., Xia, X., Raymond, P.A., 2022. The importance of hydrology in routing terrestrial carbon to the atmosphere via global streams and rivers. Proc. Natl. Acad. Sci. U. S. A. 119, e2106322119. https://doi.org/10.1073/pnas.2106322119.

Mack, M., Connon, R., Makarieva, O., McLaughlin, J., Nesterova, N., Quinton, W., 2021. Heterogenous runoff trends in peatland-dominated basins throughout the circumpolar north. Environ. Res. Commun. 3, 075006. https://doi.org/10.1088/2515-7620/ac11ed.

Marie, D., Partensky, F., Vaulot, D., Brussaard, C., 1999. Enumeration of phytoplankton, bacteria, and viruses in marine samples. Curr. Protoc. Cytom. 10, 11111–111115. https://doi.org/10.1002/0471142956.cy1111s10.

Marx, A., Dusek, J., Jankovec, J., Sanda, M., Vogel, T., van Geldern, R., Hartmann, J., Barth, J.A.C., 2017. A review of CO2 and associated carbon dynamics in headwater streams: a global perspective. Rev. Geophys. 55, 560–585. https://doi.org/10.1002/2016RG000547.

McClelland, J.W., Holmes, R.M., Peterson, B.J., Raymond, P.A., Striegl, R.G., Zhulidov, A.V., Zimov, S.A., Zimov, N., Tank, S.E., Spencer, R.G.M., Staples, R., Gurtovaya, T.Y., Griffin, C.G., 2016. Particulate organic carbon and nitrogen export from major Arctic rivers. Glob. Biogeochem. Cycl. 30, 629–643. https://doi.org/10.1002/2015GB005351.

Meybeck, M., 1993. C, N, P and S in rivers: from sources to global inputs. In: Wollast, R., Mackenzie, F., Chou, L. (Eds.), Interaction of C, N, P, and S Biogeochemical Cycles and Global Change. Springer-Verlag, Berlin, Heidelberg, pp. 163–193 NNATO ASI Series:.

Mzobe, P., Yan, Y., Berggren, M., Pilesjö, P., Olefeldt, D., Lundin, E., Roulet, N.T., Persson, A., 2020. Morphometric control on dissolved organic carbon in subarctic streams. J. Geophys. ResBiogeosciences 125, e2019JG005348. https://doi.org/10.1029/2019JG005348.

Pearce, N.J.T., Dyczko, J.M., Xenopoulos, M.A., 2022. Carbon and nutrients regulate greenhouse gas fluxes from oxic stream sediments. Biogeochemistry 160, 275–287. https://doi.org/10.1007/s10533-022-00955-3.

Pekel, J.-F., Cottam, A., Gorelick, N., Belward, A.S., 2016. High-resolution mapping of global surface water and its long-term changes. Nature 540, 418–422. https://doi.org/10.1038/nature20584.

Pokrovsky, O.S., Schott, J., Kudryavtzev, D.I., Dupré, B., 2005. Basalt weathering in Central Siberia under permafrost conditions. Geochim. Cosmochim. Acta 69, 5659–5680. https://doi.org/10.1016/j.gca.2005.07.018.

Pokrovsky, O.S., Viers, J., Shirokova, L.S., Shevchenko, V.P., Filipov, A.S., Dupré, B., 2010. Dissolved, suspended, and colloidal fluxes of organic carbon, major and trace elements in the severnaya Dvina River and its tributary. Chem. Geol. 273, 136–149. https://doi.org/10.1016/J.CHEMGEO.2010.02.018.

Pokrovsky, O.S., Shirokova, L.S., Kirpotin, S.N., Kulizhsky, S.P., Vorobiev, S.N., 2013. Impact of western Siberia heat wave 2012 on greenhouse gases and trace metal concentration in thaw lakes of discontinuous permafrost zone. Biogeosciences 10, 5349–5365.

Pokrovsky, O.S., Manasypov, R.M., Kopysov, S.G., Krickov, I.V., Shirokova, L.S., Loiko, S.V., Lim, A.G., Kolesnichenko, L.G., Vorobyev, S.N., Kirpotin, S.N., 2020. Impact of permafrost thaw and climate warming on riverine export fluxes of carbon, nutrients and metals in Western Siberia. Water (MDPI) 12, 1817. https://doi.org/10.3390/w12061817.

Raymond, P.A., Hartmann, J., Lauerwald, R., Sobek, S., McDonald, C., Hoover, M., Butman, D., Striegl, R., Mayorga, E., Humborg, C., Kortelainen, P., Dürr, H., Meybeck, M., Ciais, P., Guth, P., 2013. Global carbon dioxide emissions from inland waters. Nature 503, 355–359. https://doi.org/10.1038/nature12760.

Richey, J.E., Melack, J.M., Aufdenkampe, A.K., Ballester, V.M., Hess, L.L., 2002. Outgassing from amazonian rivers and wetlands as a large tropical source of atmospheric CO_2. Nature 416, 617–620. https://doi.org/10.1038/416617a.

Rocher-Ros, G., Sponseller, R.A., Lidberg, W., Mörth, C.-M., Giesler, R., 2019. Landscape process domains drive patterns of CO2 evasion from river networks. Limnol. Oceanogr. Lett. 4, 87–95. https://doi.org/10.1002/lol2.10108.

Rocher-Ros, G., Harms, T.K., Sponseller, R.A., Väisänen, M., Mörth, C.-M., Giesler, R., 2021. Metabolism overrides photo-oxidation in CO_2 dynamics of Arctic permafrost streams. Limnol. Oceanogr. 66, S169–S181. https://doi.org/10.1002/lno.11564.

Rosbakh, S., Hartig, F., Sandanov, D.V., Bukharova, E.V., Miller, T.K., Primack, R.B., 2021. Siberian plants shift their phenology in response to climate change. Glob. Change Biol. 27, 4435–4448. https://doi.org/10.1111/gcb.15744.

Santoro, M., Beer, C., Cartus, O., Schmullius, C., Shvidenko, A., McCallum, I., Wegmüller, U., Wiesmann, A., 2010. The BIOMASAR algorithm: An approach for retrieval of forest growing stock volume using stacks of multi-temporal SAR data. Proceedings of ESA Living Planet Symposium. Bergen, Norway.

Savenko, V.S., Pokrovskii, O.S., Dupré, B., Baturin, G.N., 2004. The chemical composition of suspended matter of major rivers of Russia and adjacent countries. Dokl. Earth Sci. 938–942.

Schneider, C.L., Herrera, M., Raisle, M.L., Murray, A.R., Whitmore, K.M., Encalada, A.C., Suárez, E., Riveros-Iregui, D.A., 2020. Carbon dioxide (CO2) fluxes from terrestrial and aquatic environments in a high-altitude tropical catchment. J. Geophys. Res. Biogeosci. 125, e2020JG005844. https://doi.org/10.1029/2020JG005844.

Serikova, S., Pokrovsky, O.S., Ala-Aho, P., Kazantsev, V., Kirpotin, S.N., Kopysov, S.G., Krickov, I.V., Laudon, H., Manasypov, R.M., Shirokova, L.S., Soulsby, C., Tetzlaff, D., Karlsson, J., 2018. High riverine CO_2 emissions at the permafrost boundary of Western Siberia. Nat. Geosci. 11, 825–829. https://doi.org/10.1038/s41561-018-0218-1.

Serikova, S., Pokrovsky, O.S., Laudon, H., Krickov, I.V., Lim, A.G., Manasypov, R.M., Karlsson, J., 2019. High carbon emissions from thermokarst lakes of Western Siberia. Nat. Commun. 10, 1552. https://doi.org/10.1038/s41467-019-09592-1.

Shirokova, L.S., Pokrovsky, O.S., Kirpotin, S.N., Desmukh, C., Pokrovsky, B.G., Audry, S., et al., 2013. Biogeochemistry of organic carbon, CO_2, CH_4, and trace elements in thermokarst water bodies in discontinuous permafrost zones of Western Siberia. Biogeochemistry 113, 573–593.

Shirokova, L.S., Payandi-Rolland, D., Lim, A., Manasypov, R.M., Allen, J., Benezeth, P., Rols, J.-L., Karlsson, J., Pokrovsky, O.S., 2020. Diurnal cycle of C concentration and emission fluxes in humic thaw ponds of frozen peatlands: application for C balance constraints. Sci. Total Environ. 737, 139671. https://doi.org/10.1016/j.scitotenv.2020.139671573-593.

Stackpoole, S.M., Butman, D.E., Clow, D.W., Verdin, K.L., Gaglioti, B.V., Genet, H., Striegl, R.G., 2017. Inland waters and their role in the carbon cycle of Alaska. Ecol. Appl. 27, 1403–1420. https://doi.org/10.1002/eap.1552.

Stanley, E.H., Casson, N.J., Christel, S.T., Crawford, J.T., Loken, L.C., Oliver, S.K., 2016. The ecology of methane in streams and rivers: patterns, controls, and global significance. Ecol. Monogr. 86, 146–171.

Striegl, R.G., Dornblaser, M.M., McDonald, C.P., Rover, J.A., Stets, E.G., 2012. Carbon dioxide and methane emissions from the Yukon River system. Glob. Biogeochem. Cycl. 26, GB0E05. https://doi.org/10.1029/2012GB004306.

Teodoru, C.R., del Giorgio, P.A., Prairie, Y.T., Camire, M., 2009. Patterns in pCO2 in boreal streams and rivers of northern Quebec, Canada. Glob. Biogeochem. Cycl. 23, GB2012. https://doi.org/10.1029/2008GB003404.

Tranvik, L., Cole, J.J., Prairie, Y.T., 2018. The study of carbon in inland waters-from isolated ecosystems to players in the global carbon cycle. Limnol. Oceanogr. Lett. 3, 41–48. https://doi.org/10.1002/lol2.10068.

Turetsky, M.R., Abbott, B.W., Jones, M.C., Anthony, K.W., Olefeldt, D., Schuur, E.A.G., Grosse, G., Kuhry, P., Hugelius, G., Koven, C., et al., 2020. Carbon release through abrupt permafrost thaw. Nat. Geosci. 13, 138–143. https://doi.org/10.1038/s41561-019-0526-0.

Vachon, D., Sponseller, R.A., Karlsson, J., 2021. Integrating carbon emission, accumulation and transport in inland waters to understand their role in the global carbon cycle. Glob. Chang. Biol. 27, 719–727. https://doi.org/10.1111/gcb.15448.

Villa, J.A., Ju, Y., Yazbeck, T., Waldo, S., Wrighton, K.C., Bohrer, G., 2021. Ebullition dominates methane fluxes from the water surface across different ecohydrological patches in a temperate freshwater marsh at the end of the growing season. Sci. Total Environ. 767, 144498.

Vonk, J.E., Tank, S.E., Mann, P.J., Spencer, R.G.M., Treat, C.C., Striegl, R.G., Abbott, B.W., Wickland, K.P., 2015. Biodegradability of dissolved organic carbon in permafrost soils and aquatic systems: a meta-analysis. Biogeosciences 12, 6915–6930. https://doi.org/10.5194/bg-12-6915-2015.

Vonk, J.E., Tank, S.E., Walvoord, M.A., 2019. Integrating hydrology and biogeochemistry across frozen landscapes. Nat. Commun. 10, 5377. https://doi.org/10.1038/s41467-019-13361-5.

Vorobyev, S.N., Pokrovsky, O.S., Kolesnichenko, L.G., Manasypov, R.M., Shirokova, L.S., Karlsson, J., Kirpotin, S.N., 2019. Biogeochemistry of dissolved carbon, major, and trace elements during spring flood periods on the Ob River. Hydrol. Proc. 33, 1579–1594. https://doi.org/10.1002/hyp.13424.

Vorobyev, S.N., Karlsson, J., Kolesnichenko, Y.Y., Korets, M.A., Pokrovsky, O.S., 2021. Fluvial carbon dioxide emission from the Lena River basin during the spring flood. Biogeosciences 18, 4919–4936. https://doi.org/10.5194/bg-18-4919-2021.

Wallin, M.B., Grabs, T., Buffam, I., Laudon, H., Ågren, A., Öquist, M.G., Bishop, K., 2013. Evasion of CO2 from streams – the dominant component of the carbon export through the aquatic conduit in a boreal landscape. Glob. Change Biol. 19, 785–797. https://doi.org/10.1111/gcb.12083.

Xiao, Q., Xu, X., Duan, H., Qi, T., Qin, B., Lee, X., Hu, Z., Wang, W., Xiao, W., Zhang, M., 2020. Eutrophic Lake Taihu as a significant CO_2 source during 2000–2015. Water Res. 170, 115331. https://doi.org/10.1016/j.watres.2019.115331.

Xiao, Q., Hu, Z., Hu, C., Islam, A.R.M.T., Bian, H., Chen, S., Liu, C., Lee, X., 2021. A highly agricultural river network in Jurong Reservoir watershed as significant CO_2 and CH_4 sources. Sci. Total Environ. 769, 144558. https://doi.org/10.1016/j.scitotenv.2020.144558.

Yamamoto, S., Alcauskas, J.B., Crozier, T.E., 1976. Solubility of methane in distilled water and seawater. J. Chem. Eng. Data. 21, 78–80.